Chapter 5: Racemic Resolution in Molecular Materials

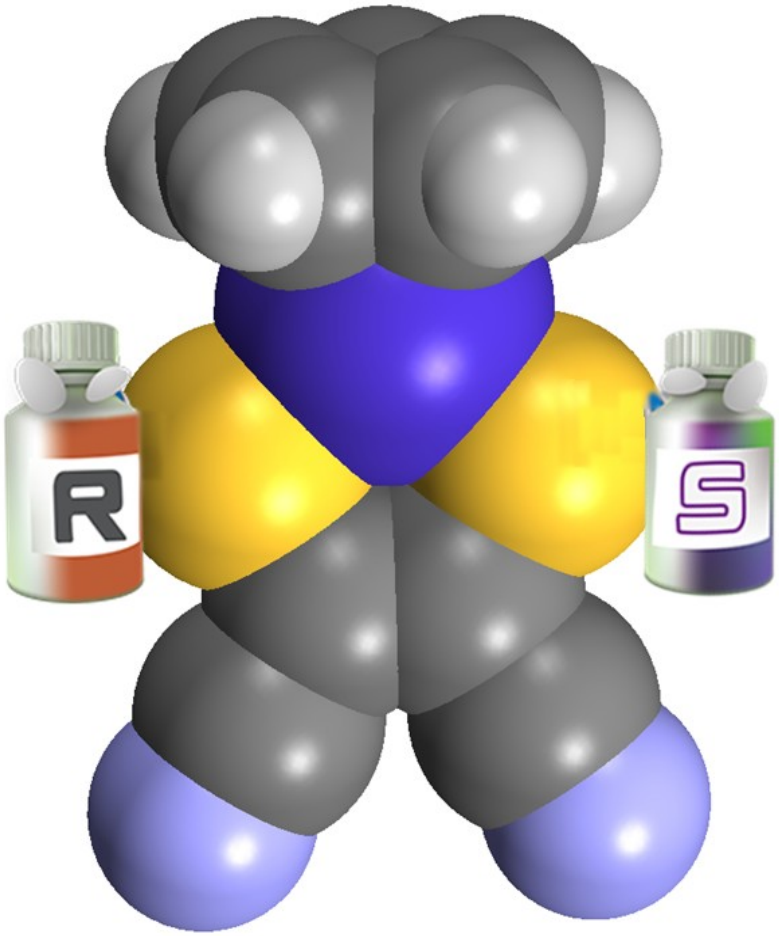

The role of chirality is no more limited to biological structures, but is exploited in enantio- selective synthesis and asymmetric catalysis [1], along with technology conscious designing of chiral molecular magnets [2] and optoelectronics [3].
Introduction of chirality in the structure is normally carried out by employing chiral ligands or by the use of chiral solvents, chiral ionic liquids, or even by manipulating geometrical structure in achiral ligands [4]. One technologically important attribute of chiral compounds is the generation of helicity or helical chain network during their Self-assembly process and crystallization.

Crystallization is the self-assembly and self-recognition of atoms, ions, and molecules being packed precisely from 1D to 3D order due to rearrangement of intermolecular forces. Self-assembly is one of the most powerful methods for preparing different scales of functional materials. Chiral information can also pass from single molecules to supramolecular assemblies and then to macroscopic superstructures through a self assembly process.

The crystallization of racemates into chiral space groups is extremely rare. The use of crystallization in this chapter is however, limited by the observed behavior of chiral molecules isolated from racemic solutions. Three major outcomes are possible during crystallization of a racemic solution: (i) a racemic compound is formed in which each crystal contains a 1:1 mixture of enantiomers, (ii) a *conglomerate* appears, which is a physical mixture of homochiral crystals; (iii) a solid solution is formed in which each crystal is heterochiral i.e. *pseudoracemate*. Only the conglomerate implies spontaneous resolution [5].
Spontaneous optical resolution is an interesting chiral-recognition event in which racemic compounds are crystallized to form homochiral assemblies (conglomerates) of individual enantiomers [6]. Spontaneous resolution is an unusual phenomenon, though a large number of chiral organic and organo–inorganic hybrid solids have been synthesized since the well known experiment on ammonium sodium tartrate by Louis Pasteur [7] in 1848. Thus, optically pure compounds are produced without any assistance from chiral environments. Because of significant loss in entropy only 10% chiral compounds had been resolved by crystallization method [8].

For most materials, solid crystallizing as a racemic compound is by far more common than as a racemic conglomerate indicating the preference of heterochiral to homochiral interactions in the packing energy (enthalpy,ΔH) or the packing efficiency (entropy, $T \Delta S$) in the process of crystallization [9].

Although the formation of conglomerates has not yet been fully understood, comparatively strong and directional coordination bonds and non-covalent interactions including hydrogen bonding and π–π stacking undoubtedly play a key role in chiral recognition [10] or in other words nature of "synthons" responsible for the induction of homo-helicity in crystals.

Motivation: Is it possible to observe spontaneous resolution during crystallization? We discuss our self-assembly driven crystallization to produce *'conglomerates' (need more understanding)* due to (a) presence of Cl^- anion (b) change in auxiliary ligand.

Part-I: Chloride anion assisted Resolution of chiral cobalt compounds

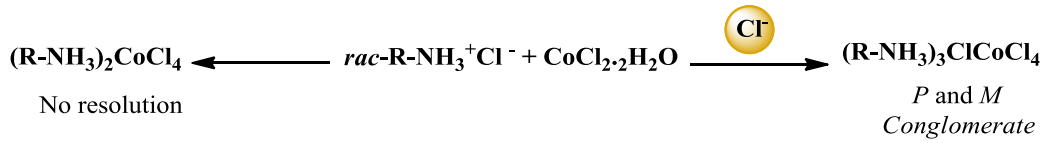

Abstract:

In this chapter (part I), we have synthesized four new cobalt based compounds, from substituted benzylamines as shown below, with a general formula $(R\text{-}NH_3)_nCl_xCoCl_4$, [where, $R\text{-}NH_3$ = (*R*)- (+)-4-chloro methyl benzylamine (**1*R***) and (*S*)- (-)-4-chloro methyl benzylamine (**1*S***), (±) 4-fluro methyl benzylamine (**2**), (*R*)- (+)- methyl benzylamine (**3*R***),; x= 0, 1 and n=2, 3]. Due to crystallization of free chlorine ion in the compounds **1*R***, **1*S*** and **3*R*** variation in number of ligands in final the formulae was observed. These compounds were investigated for thermal analyses and single crystal XRD spectroscopy. We could not crystallize compound **1**, *racemic* (±)-4- chloro methyl benzylamine, due to spontaneous resolution and separate crystallization of isomers i.e. compound **1*R*** and **1*S***, conglomerate formation. Single crystal XRD studies on these compounds revealed that inclusion of chloride anion in (1) resulted in the formation of a new 'acutely anisotropic' synthon, $Cl^{\cdots}N$ interaction, for driving spontaneous resolution of the racemic amine. Interestingly, compound **2** crystallized devoid of such synthon and hence contain both isomers in a crystal structure.

Compound **1*R***, **1*S*** and **3*R*** are crystallized in monoclinic crystal system with chiral (polar) space group, $P2_1$, and unit cell dimensions for **1*R*** a=13.9263(14) Å, b= 7.5981(6) Å, c = 15.8322(13) Å, β= 95.173(6)°, V= 1668.4(3) $Å^3$ and Z = 2; for **1*S*** a = 13.7886(2) Å, b = 7.55490(10) Å, c = 15.5888(2) Å, β = 94.963(1)°, V= 1617.82(4) $Å^3$ and Z = 2 and for **3*R*** a=13.9448(2) Å, b = 7.5033(1) Å, c = 14.4057(2) Å, β= 98.471(10)°, V= 490.85(4) $Å^3$ and Z = 2. Compound **2** crystallized in triclinic crystal system with non chiral (non polar) space group, *P-1*, and unit cell dimensions: a = 7.1784(1) Å, b = 10.5916(1) Å, c = 14.2341(1) Å, α = 90.529(1), β = 92.765(1), γ = 98.009(1), V = 1070.29 $Å^3$ and Z = 2.

5.1 Introduction

Chirality and helical structures are interwoven in literature but are not limited to each other. The most prominent examples of natural helices with out chirality are double-helical *β*-DNA and with chirality are *α*-helical structures found in proteins [11]. Constructing and regulating helicity in molecular structures using chiral molecules is of great importance for exploring new properties and hence functional materials [12].

The most important property of a helix is its 'spinning axis' which can be right-handed (plus, *P*) or left-handed (minus, *M*), depending on whether the rotation is clockwise or anticlockwise when a helicate is considered to wind from the eye of the viewer towards a distant point from the viewer [13]. Right- and left-handed helices are obtained in equal amounts for *meso*-compound when normally achiral or racemic building blocks are employed [14] with crystallization in centrosymmetric space group. Presence of equal amount of right- and left-handed separate crystals (or polycrystals) in a bulk compound can some time mis-concluded (with out detailed investigation) as *meso* compound.

For the design and constructions of single stranded helical structures, the most successful approach is to use enantiopure ligands as building blocks [15]. However, sometimes spontaneous resolution occurs during the crystallization which yields a conglomerate [16]. That means, conglomerate-forming system can use racemate mixture for spontaneous resolution of enantiomers. But which racemic mixture will undergo conglomarate formation is a challenging question? We realized investigation of a proper synthon can help in generating conglomerates.

An effort was made for the design and construction of helical structures using the racemic ligands *α*-(±)-methyl benzylamine and derivatives (containing equal amounts of *S* and *R* enantiomers), and enantiopurically pure (*S*) and (*R*) ligands as building blocks. Investigation for the correlation between chirality of the building blocks, synthons and helicity of the structures is reported. Interestingly, we observed spontaneous resolution due to formation of homochiral helical chains driven by novel $Cl^{-}\cdots HN$ synthons i.e. hydrogen bonding and crystallisation of free chlorine atom. The observed 'synthon' is a

result due to “inclusion” of chloride anion during crystallization in the company of $CoCl_2$ by racemic amines.

5.2 Experimental

5.2.1 Materials and Methods:

All chemicals and solvents were of analytical grade reagents. (*R*)- (+)-methyl benzyl amine, (±) 4-fluro methyl benzylamine, (*R*)-(+)-4-chloro-α-methyl benzylamine, (*S*)-(-)4-chloro-α-methyl benzylamine and cobalt (II) chloride were from Aldrich; conc. hydrochloric acid (Qualigens) and ethyl alcohol (Baroda chemicals) were used without further purification.

5.2.2 Syntheses of compounds:

A general methodology of cobalt based compound preparation/syntheses is mentioned in scheme-5.1.

Scheme: 5.1

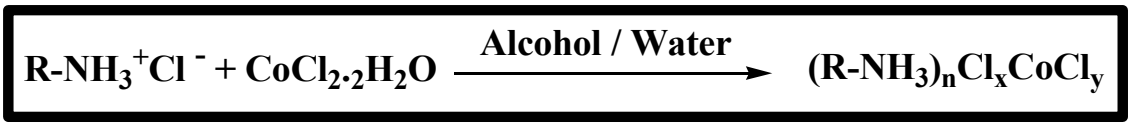

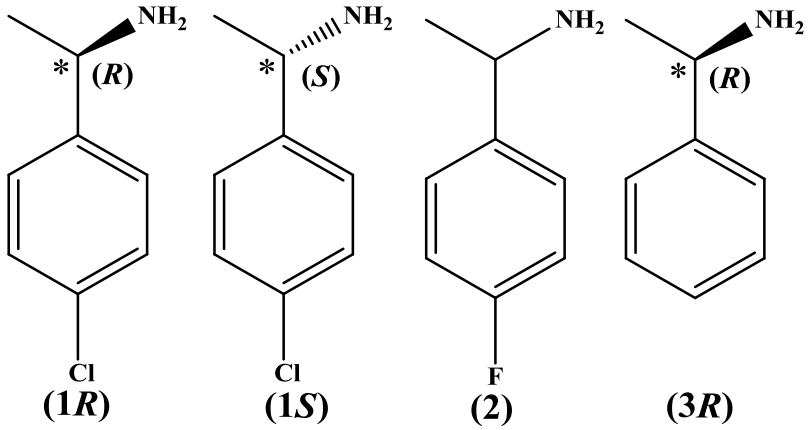

An acidified ethanolic solution (10 mL) containing (±) 4-fluro methyl benzylamine (0.2 mmol) and cobalt (II) chloride (0.2 mmol) were mixed and refluxed for three hours. The resulting dark-blue coloured solution was evaporated to dryness and precipitate washed using ether. It was then recrystallized using 2-3 ml ethanol. The solution left to stand at low temperature. Dark blue plate-shaped crystals of **2** suitable for X-ray diffraction were obtained within 1 week.

Compound **1*R*, 1*S*** and **3*R*** were obtained using a similar method to that of **2**, except that, (*R*)-(+)-4-chloro methyl benzylamine, (*S*)-(-)-4-chloro methyl benzylamine ligands and (*R*)-(+)-methyl benzyl amine were used. Yield: ~ 54% for pure crystals.

5.3 Result and Discussions

5.3.1 FT-IR:

The vibrational spectra for **1*R***, **1*S***, **2** and **3*R*** (Figure 5.1) were recorded in the range of 4000-400cm^{-1}. Formation of the compounds indicated by the observation of broad band in the range 3165-2952 cm^{-1} due to merging of the $-NH_3^+$ stretching modes with aromatic C-H stretching modes. The strength of M (II)-N-H bond and hydrogen bond (N-H---Cl) determines the position of asymmetric stretching modes of N-H ($-NH_3^+$ group) and shifts to lower wavenumbers [17]. Bands at 2978 and 2949cm^{-1} indicates the asymmetric stretching due to terminal methyl ($-CH_3$) group. Intense band in range of 2562-2555 cm^{-1} assigned to the combination modes of deformation and rocking modes of N-H ($-NH_3^+$ group).

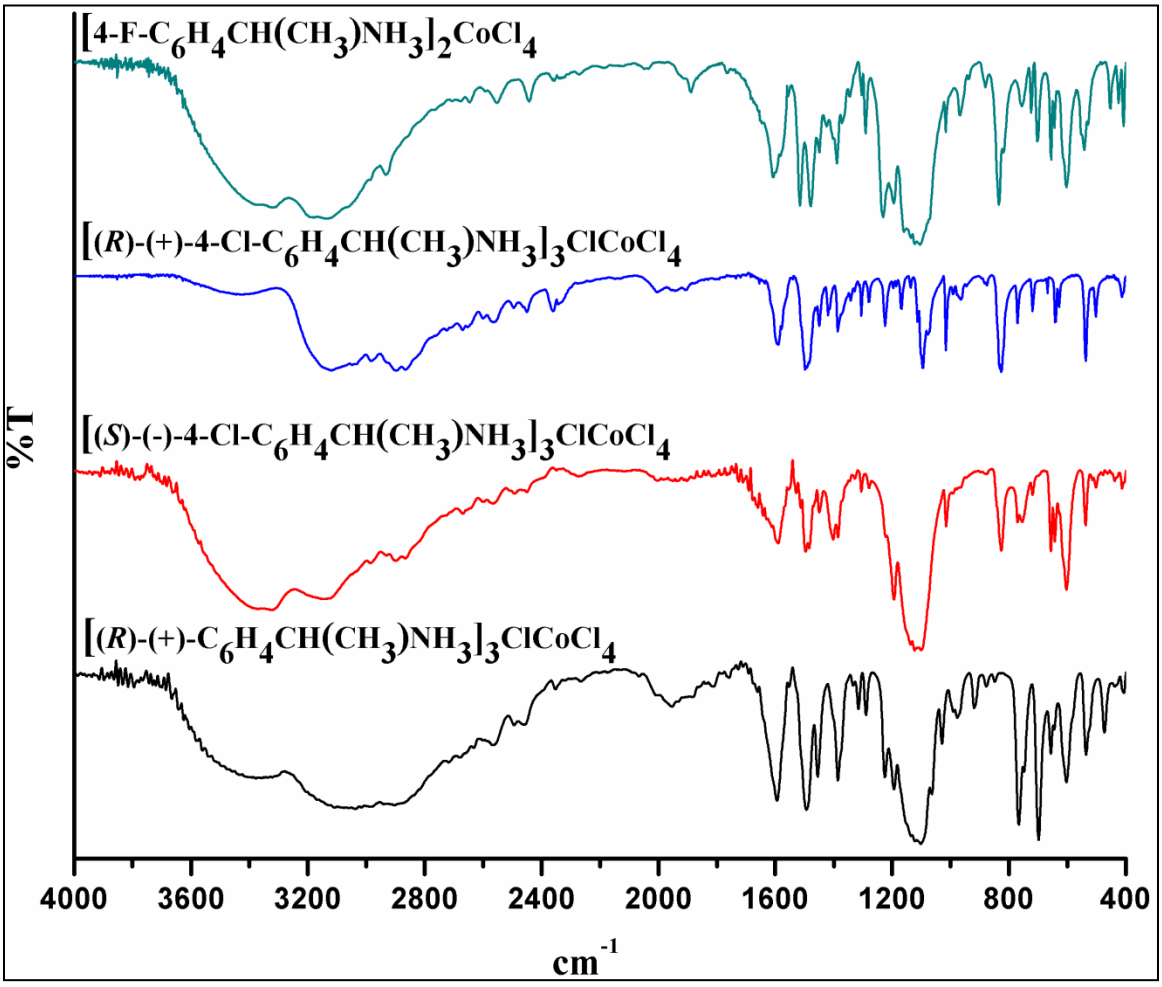

Fig. 5.1: FT-IR spectra of compounds 1*R*, 1*S*, 2 and 3*R*

Compound 1*R*- FT-IR (KBr): 3117 (vs), 3040 (vs), 2983 (s), 2900 (vs), 2864 (vs), 2667 (m), 2650 (w), 2605 (m), 2564 (s), 2495 (m), 2445 (s), 1654 (w), 1637 (w), 1613 (s), 1592 (vs), 1577 (s), 1561(m), 1539(w), 1497 (vs), 1490 (vs), 1483 (s), 1461(w), 1450 (s), 1418 (s), 1385 (vs), 1373 (s), 1342 (m), 1327 (w), 1305 (s), 1279 (s), 1224 (vs), 1197 (m), 1186 (m), 1170 (s), 1139 (m), 1114 (s), 1095 (vssh), 1076 (vs), 1015 (vssh), 990(m), 964 (m), 944 (w), 884(w), 875 (m), 833(vssh), 825(vssh), 770 (vs), 719 (vs), 667 (s), 640 (vs), 628 (s), 536 (vssh), 518(w), 502 (vs) and 413 (s) cm^{-1}.

Compound 1*S*- FT-IR (KBr): 3121 (vs), 3036 (vs), 2987 (s), 2904(vs), 2864 (vs), 2671 (m), 2646 (w), 2601 (m), 2564 (s), 2491 (m), 2449 (s), 1658 (w), 1640 (w), 1615 (m), 1590 (vs), 1570 (m), 1542 (w), 1496 (vs), 1486 (vs), 1464(m), 1450 (s), 1414 (s), 1402 (vs), 1384 (vs), 1371(m), 1344(w), 1328(m), 1307(m), 1280 (m), 1224 (s), 1195(s), 1139(vs), 1124(vs), 1099 (vs) , 1015(s), 988(w), 967(w), 880(w), 839 (s), 825 (vssh), 770 (s), 754 (s), 719 (m), 660(s), 644 (s), 628(m), 603 (vs), 537(vs), 515 (m), 502(m) and 412 (m) cm^{-1}.

Compound 2- FT-IR (KBr): 3400 (vs), 3032 (vs), 2681 (m), 2586 (w), 1611 (vs), 1552 (m), 1496 (s), 1457 (s), 1386 (s), 1316 (m), 1291 (m), 1225 (ssh), 1169 (w), 1088 (s), 1064 (s), 1029 (m), 976 (w), 918 (w), 768 (ssh), 700 (vssh), 582 (w), 536 (s) and 476 (m) cm^{-1}.

Compound 3*R*- FT-IR (KBr): 3380 (vs), 3316 (vs), 3185 (s), 3136 (vs), 2933 (s), 2648 (m), 2550 (s), 2440 (s), 1891 (s), 1764 (w), 1606 (vs), 1580 (s), 1556 (w), 1518 (vs), 1477 (vs), 1450 (m), 1424 (w), 1387 (s), 1367 (m), 1344 (m), 1305 (m), 1290 (s), 1230 (vs), 1195 (s), 1161 (vs), 1137 (vs), 1122 (s), 1103 (vs), 1070 (s), 1017(s), 967(s), 937 (w), 880 (m), 834 (vssh), 817 (vs), 755 (s), 725 (s), 704 (vs), 656 (vs), 643 (s), 605 (vssh), 544 (vs), 452 (s), 424 (s) and 407 (s) cm^{-1}.

Out of plane bending modes of $–NH_3^+$ were observed at 885-879 cm^{-1} while rocking modes of $–NH_3^+$ were observed at 1307 and 1278-1291 cm^{-1}. C-C ring stretching modes were observed at 1454-1604 cm^{-1}. C-N stretching mode was observed at 1333-1347 cm^{-1}. Bands at 1062- 1238 cm^{-1} assigned to the in plane C-H deformation of ring while bands

at 690-771 cm^{-1} assigned to the out of plane C-H deformation mode. -CH_2 rocking mode was observed at 910 cm^{-1}.

5.3.2 Elemental analyses:

The calculated and observed elemental analyses were consistent with the formulae $(R\text{-}NH_3)_nCl_xCoCl_4$ (x = 0, 1 and n= 2, 3)

Compound 1*R*: Anal. Calc. for $C_{24}H_{33}Cl_8N_3Co$: C, 40.79; H, 4.67; N, 5.95%. **Found:** C, 40.85; H, 4.70; N, 5.87%.

Compound 1*S*: Anal. Calc. for $C_{24}H_{33}Cl_8N_3Co$: C, 40.79; H, 4.67; N, 5.95%. **Found: C**, 40.68; H, 4.61; N, 5.90%.

Compound 2: Anal. Calc. for $C_{16}H_{22}Cl_4F_2N_2Co$: C, 39.90; H, 4.57; N, 5.82% **Found**: C, 39.56; H, 4.61; N, 5.80%.

Compound 3*R*: Anal. Calc. for $C_{24}H_{36}Cl_5N_3Co$: C, 47.80; H, 5.97; N, 6.97%. **Found:** C, 47.70; H, 6.30; N, 6.86%.

5.4 Thermal Studies

5.4.1 Thermo Gravimetry/Differential Thermal Analysis (TG/DTA):

TG/DTA of cobalt based compounds was performed on the powdered samples. Figure 5.2 showed the thermal analyses of compounds **1*R***, **1*S***, **2** and **3*R***. Compounds **1*R*** and **1*S*** are enantiomers hence follow similar degradation pathways while **2** and **3*R*** follow similar degradation pathways (Figure 5.3), as tabulated below. Thermo-gravimetric studies were carried out for the all the compounds in nitrogen atmosphere in the 303-850 K temperature range.

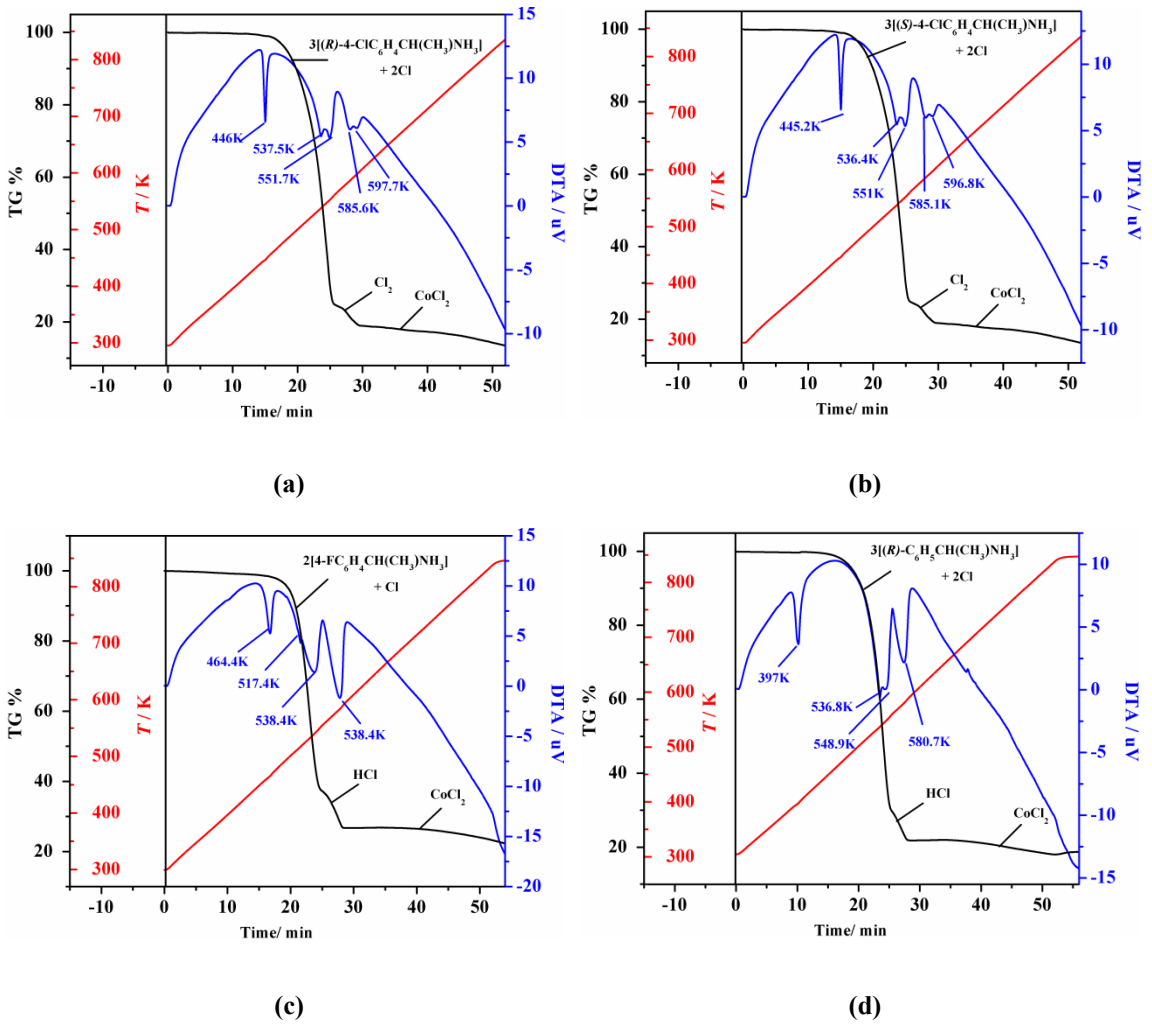

Fig. 5.2: TG/DTA thermogram for compounds 1*R* (a), 1*S* (b), 2 (c) and 3*R* (d)

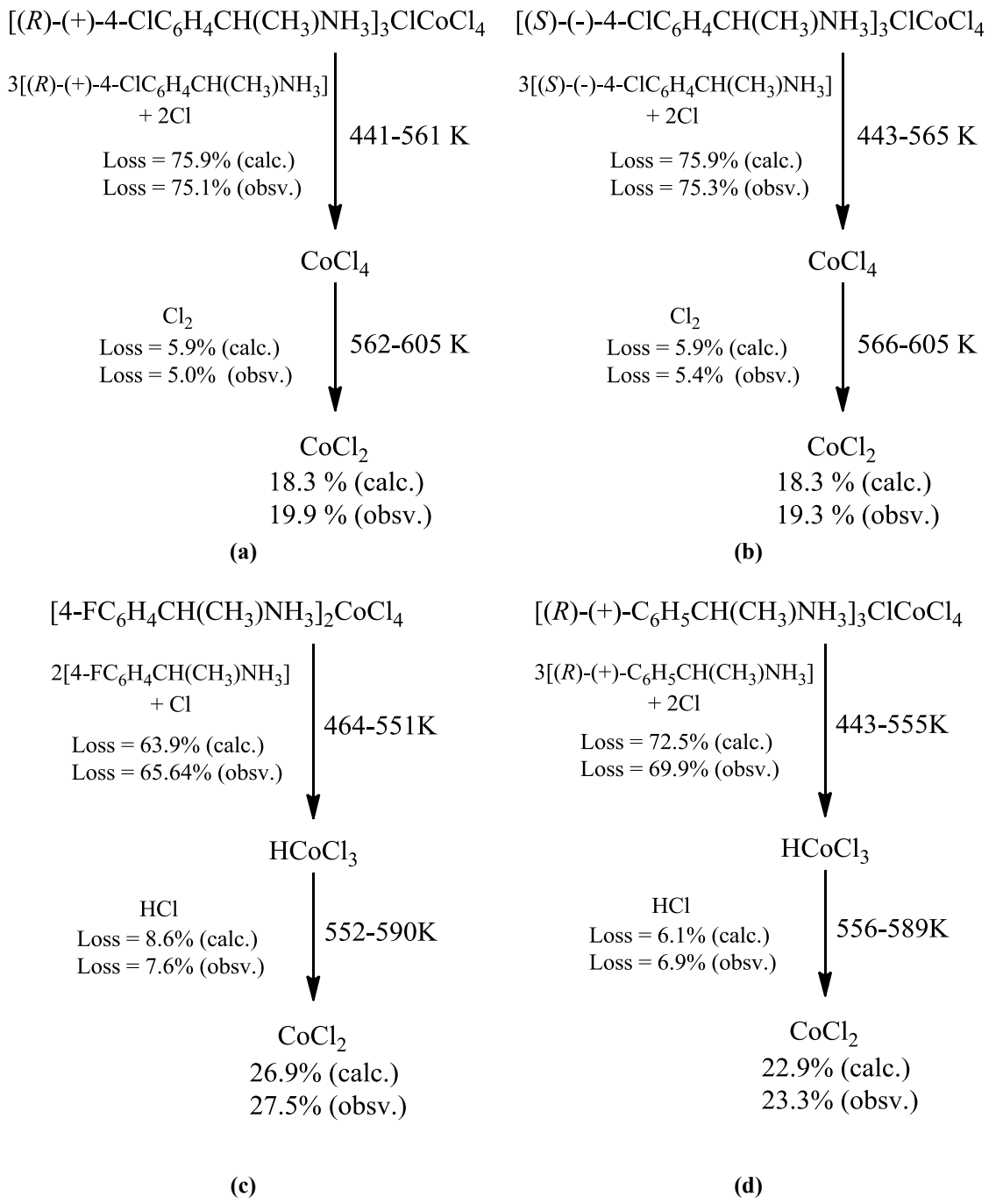

Fig. 5.3: Degradation pathway for compounds 1*R* (a), 1*S* (b), 2 (c) and 3*R* (d)

The multi-step decomposition patterns of **1*R***, **1*S***, **2** and **3*R*** are quite similar where decomposition steps are accompanied by the gradual loss of number of chloride ion molecules along with the ligand molecules, followed by mass loss of HCl molecule or loss of Cl_2.

Three organic ligands and two chlorine ions decomposes gradually in the range of 441-561 K for **1*R*** (Obsd. 75.1 Calcd. 75.9%) and 443-565 K for **1*S*** (Obsd. 75.3%, Calcd. 75.9%) and 443-555 K for **3** (Obsd. 69.9%, Calcd. 72.5%) while two organic ligands and one chlorine ion get decomposes in the range of 464-551K for **2** (Obsd. 65.6%, Calcd. 63.9%). Probable formation of $HCoCl_3$ was observed in case of **2** and **3*R*** which on further heating give loss of HCl molecule while $CoCl_4$ formation was observed in case of **1*R*** and **1*S*** which give loss of Cl_2 on further heating. The remaining product in all compounds at high temp is probable $CoCl_2$ [**1*R***- Obsd. 19.9%, Calcd. 18.3%), (for **1*S***- Obsd. 19.3%, Calcd. 18.3%), (for **2**- Obsd. 27.5%, Calcd. 26.9%) and (for **3*R***- Obsd.23.3%, Calcd. 22.9%)].

The DTA curves for all compounds showed solid to liquid phase transition which was also confirmed by monitoring melting points externally. Decomposition of the compound took place with two endothermic peaks at 537.5 K and 551.7 K for **1*R*** and 536.4 K and 551K for **1*S***, 517.4 K and 538.4 K for **2** and 536.8 K and 548.9 K for **3*R*** corresponding to loss of ligand and Cl^- ions. Two endothermic peaks observed at 585.6 K and 597.7K in case of **1*R*** and 585.1 K and 596.8K in case of **1*S*** while single endothermic peaks observed at 538.4 K in case of **2**and 580.7 K in case of **3*R***.

5.5 Crystal structure

5.5.1 Single Crystal X-ray Diffraction

Single crystal XRD confirms the formation of compounds and crystals. The molecular structure of **1*R***, **1*S***, **2** and **3*R*** are shown in Figure 5.4. The selected bond lengths, angles and hydrogen bonds of the title compound are listed in Table 5.1.

Table 5.1: Crystal structure and refinement parameters for 1*R*, 1*S*, 2 and 3*R*

	1*R*	**1*S***	**2**	**3*R***
Empirical formula	$C_{24}H_{33}Cl_8CoN3$	$C_{24}H_{33}Cl_8CoN3$	$C_{16}H_{22}Cl_4CoF_2N_2$	$C_{24}H_{36}Cl_5CoN_3$
Formula weight	706.06	706.06	481.09	602.74
Wavelength	0.71073 Å	0.71073 Å	0.71073 A	0.71073 A
Crystal system	Monoclinic	Monoclinic	Monoclinic	Monoclinic
Space group	$P2_1$	$P2_1$	*P-1*	$P2_1$
Unit cell dimensions	a = 13.7886(2) Å b = 7.55490(10) Å c = 15.5888(2) Å α = 90° β = 94.963(1)° γ = 90°	a = 13.9263(14) Å b = 7.5981(6) Å c = 15.58322(13) Å α = 90° β = 95.173(6)° γ = 90°	a = 7.1784(1) Å b = 10.5916(1) Å c = 14.2341(1) Å α = 90.529(1)° β = 92.765(1)° γ= 98.009(1)°	a = 13.9448(2) Å b = 7.5033(1) Å c = 14.4057(6) Å α = 90° β = 98.471(10) ° γ= 90°
Volume	1617.82(4) $Å^3$	1668.4(3) $Å^3$	1070.29(2) $Å^3$	1490.85(4) $Å^3$
Z	2	2	2	2
Density (calculated)	1.449 Mg/m^3	1.405 Mg/m^3	1.493 Mg/m^3	1.343 Mg/m^3
Absorption coefficient	1.210 mm^{-1}	1.173 mm^{-1}	1.320 mm^{-1}	1.041 mm^{-1}
Reflections collected	18805	15274	26224	15614
Independent reflections	10842[R(int) = 0.0186]	8142 [R(int) = 0.0325]	8471 [R(int) = 0.0289]	9553[R(int) = 0.0233]
Refinement method	Full-matrix least-squares on F^2	Full-matrix least-squares on F^2	Full-matrix least-squares on F^2	Full-matrix least-squares on F^2
Data / restraints / parameters	7286/1/260	8142 / 1 / 325	8471 / 0 / 298	9553 / 1 / 298
Goodness-of-fit on F2	1.012	1.019	1.032	1.004
Final R indices [I>2sigma(I)]	R1 = 0.0264 wR2 = 0.0569	R1 = 0.0401 wR2 = 0.0801	R1 = 0.0415 wR2 = 0.0977	R1 = 0.0378 wR2 = 0.0769
R indices (all data)	R1 = 0.0309 wR2 = 0.0587	R1 = 0.0622 wR2 = 0.0894	R1 = 0.0620 wR2 = 0.1089	R1 = 0.0495 wR2 = 0.0816
Absolute structure parameter	0.011(7)	0.004(14)		0.012(10)

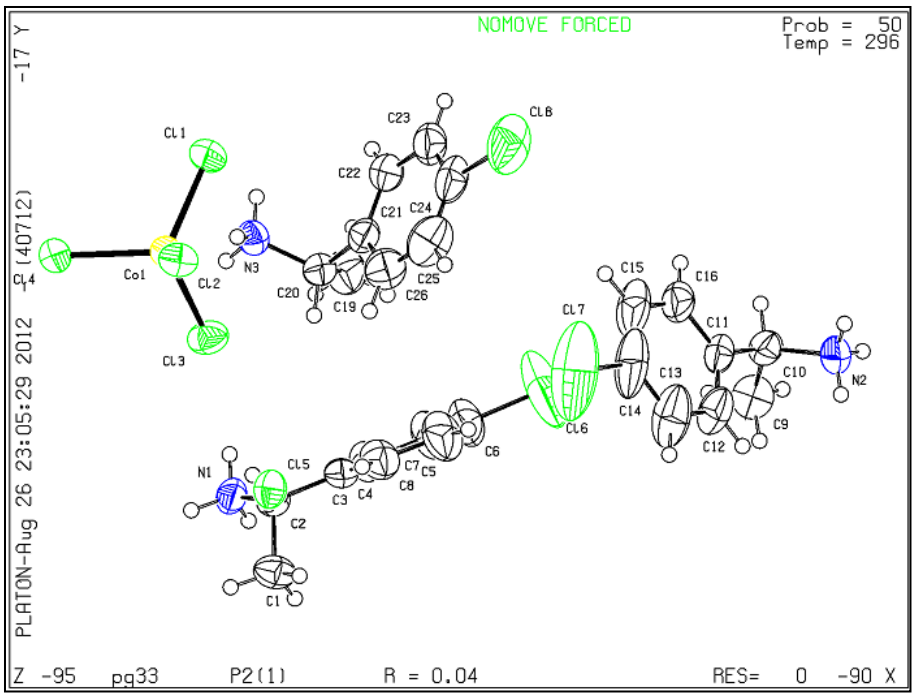

(a)

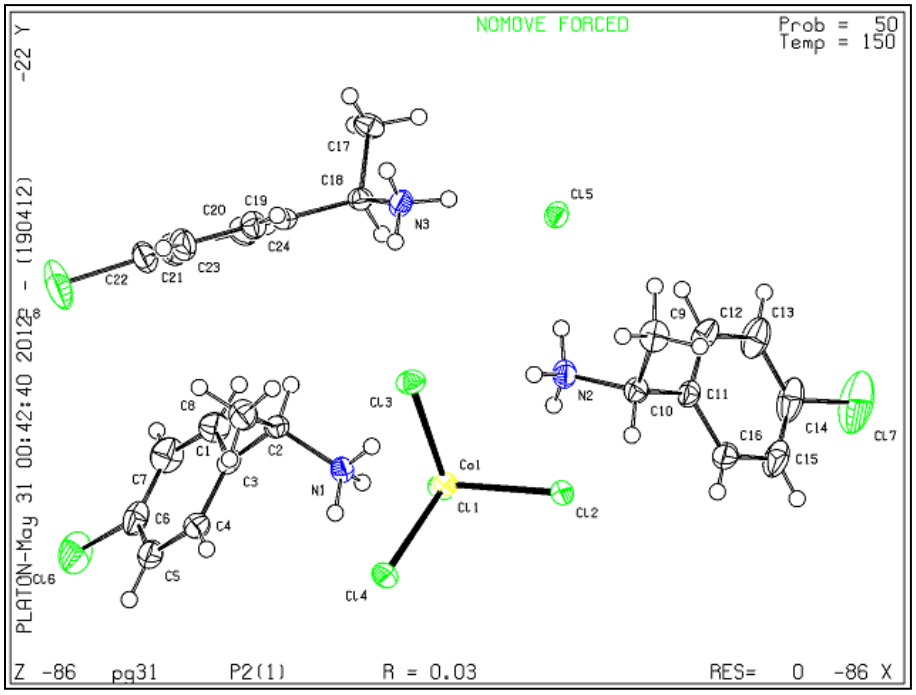

(b)

Fig. 5.4: Molecular view of compounds 1*R* (a) and 1*S* (b) having thermal ellipsoid are drawn at the 50% probability level

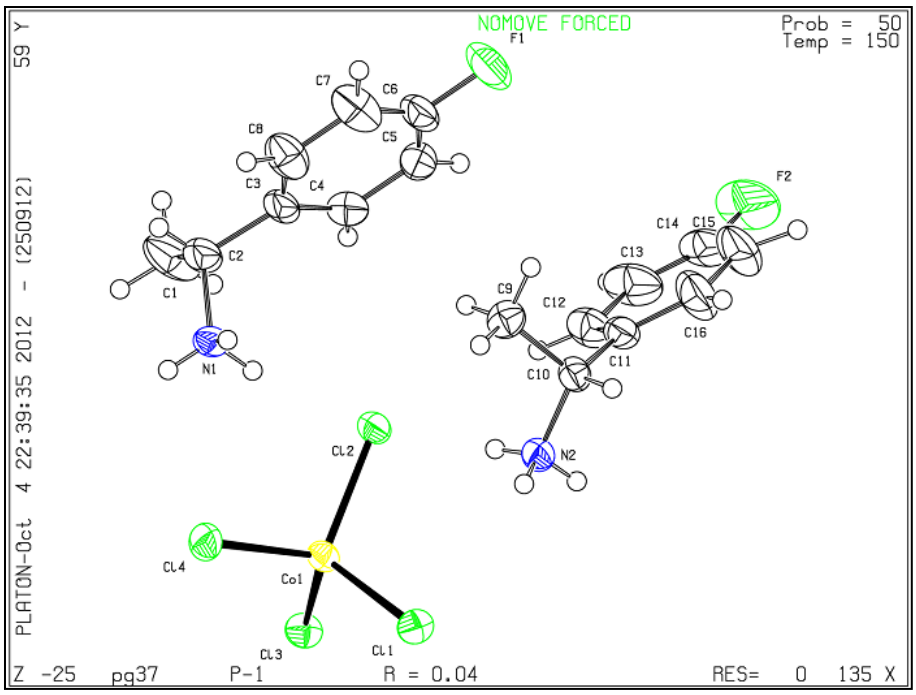

(c)

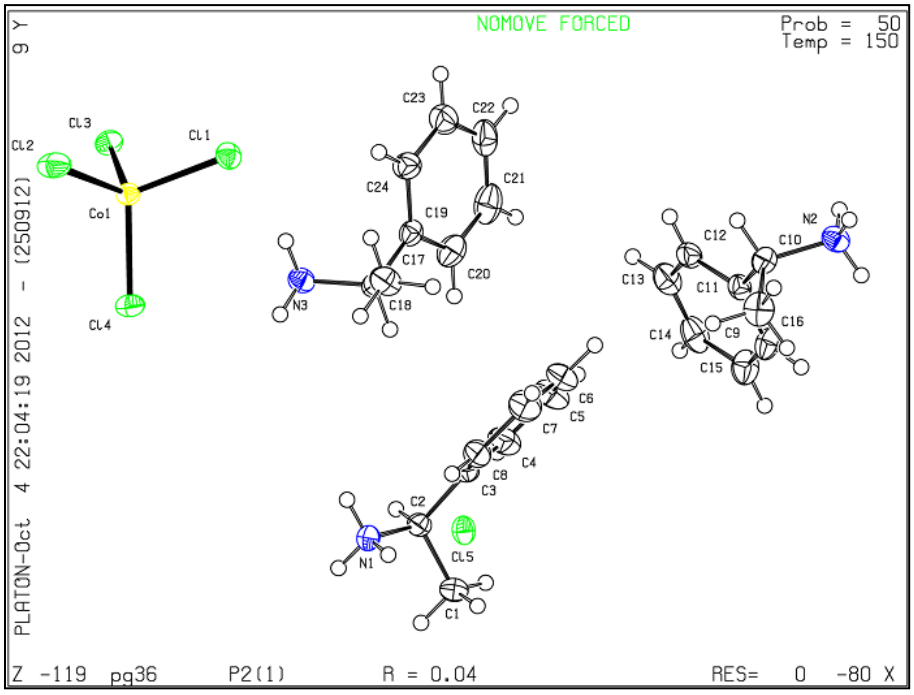

(d)

Fig. 5.4: Molecular view of compounds 2 (c) and 3*R* (d) having thermal ellipsoid are drawn at the 50% probability level

Compounds **1*R*** and **1*S*** (Figure 5.4-a,b) crystallize in the non-centro-symmetric (chiral) monoclinic crystal system with space group $P2_1$. Unit cell dimensions for **1*R***: a =13.9263(14) Å, b = 7.5981(6) Å, c = 15.8322(13) Å, β = 95.173(6)°, V = 1668.4(3) Å^3. Unit cell dimensions for **1*S***: a = 13.7886(2) Å, b = 7.5549(1) Å, c = 15.5888(2) Å, β = 94.963(1)°, V = 1617.82(4) Å^3 and Z = 2. Compound **2** (fig.5.4c) crystallizes in the centro-symmetric triclinic space group $P\bar{1}$with cell dimensions a = 7.1784(1) Å, b = 10.5916(1) Å, c = 14.2341(1) Å, α = 90.529(1), β = 92.765(1), γ = 98.009(1), V = 1070.29 Å^3 and Z = 2.

In all these structures $CoCl_4^{2-}$ anions assume tetrahedral geometry with the average Cl-Co-Cl trans bond angles being in the range of 106º-115º. The major difference between conglomerate crystals, **1*R***, **1*S***, and **2** is asymmetric unit. The asymmetric units of **1*R*** and **1*S*** consist of three ammonium cations, one $CoCl_4^{2-}$ ion along with one free chloride anion while asymmetric unit of **2** consists of two benzylammonium cations and one $CoCl_4^{2-}$anion, (A_2CoCl_4).

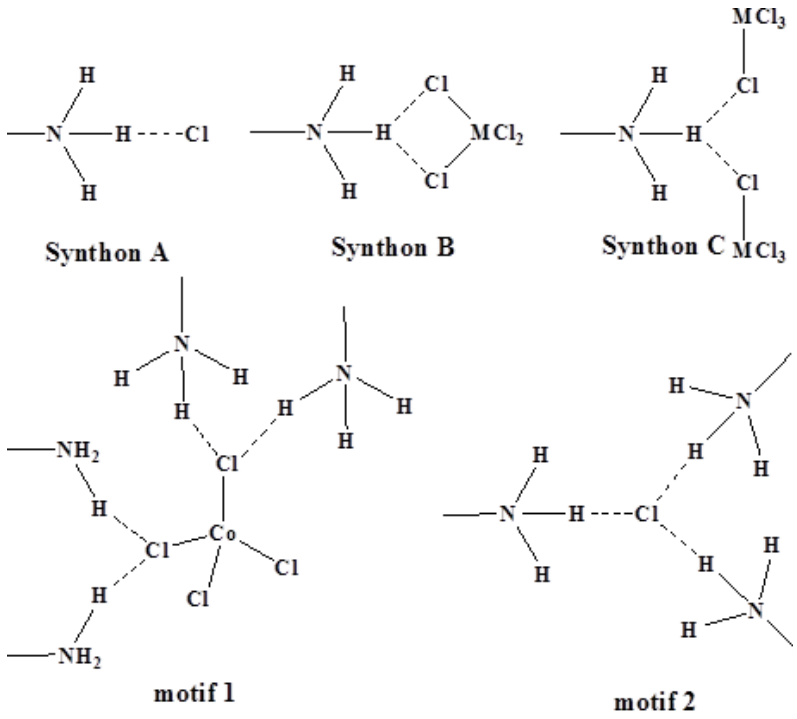

Scheme 5.2: Hydrogen-bonding synthons and connectivity motifs found in amine and metal salt [18].

Different synthons and motifs observed in present set of compounds are listed in Scheme 5.2. Close look at the crystal structures of **1*R*** and **1*S*** showed hydrogen bonding

interactions in the form of synthons A and C (Scheme 5.2). The free chloride anion present in these two crystals is involved in classical hydrogen bonds with the three 4-chloro-α-phenylethylammonium cations (synthon A; motif 2). While synthon C is shown by $[CoCl4]^{2-}$ anion, by acting four-connecting node with two bifurcated hydrogen bonds N-H···MX4···N-H (motif 1). This makes slight distortion in $[CoCl4]^{2-}$ tetrahedra. The $[CoCl4]^{2-}$ and Cl^{-} anions form 2-D layer structure with two independent circuits A and B with 4-chloro-*α*-phenyleneethyl ammonium cations as shown in Figure 5.5.

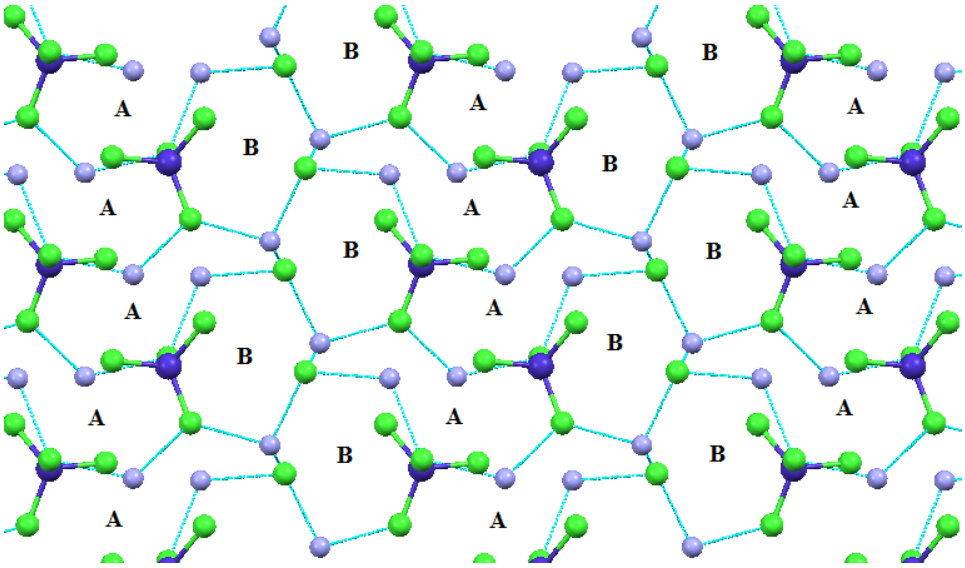

Fig. 5.5: 2D sheet arrangement adopted by 1*R*/1*S* with two independent circuits A and B, propagated by N–H···Cl–Co and N–H···Cl hydrogen bonds

In contrast, in the case of compound **2**, $CoCl_4^{2-}$is hydrogen bonded to the benzylammonium N–H groups by synthon B. The strong hydrogen bonding interaction results in a 1-D linear helical chain arrangement of the cations and anions as shown in Figure 5.6.

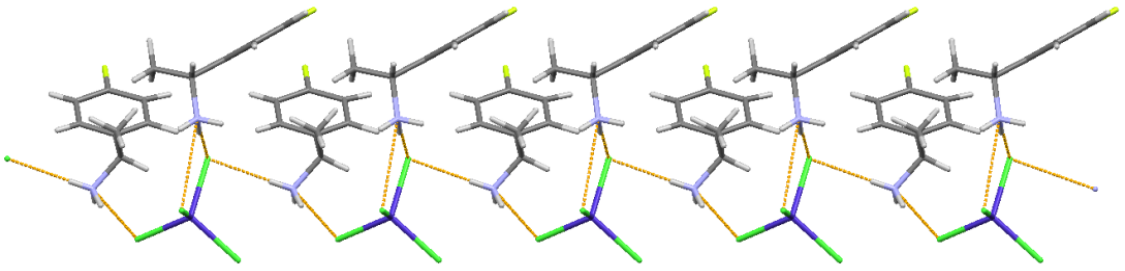

Fig. 5.6: Linking of 4-F phenylethylammonium cations and tetrachloro cobaltate anions through N–H···Cl hydrogen-bonded contacts to form a 1-D chain (tapes) of alternating cations and anions in compound 2

The hydrogen bonding interactions due to synthons A and C for compound **1*R*** and **1*S***, and synthon B for compound **2** dictate helicity, as shown in Figure 5.7 a-c. Usually, crystals with structural helicity are found to be racemic or in low enantiomeric excess when achiral or racemic building blocks are used, since both the left- and right-handed helical structures are produced with equal probability. In compound **2,** with synthon B, anti-parallel/racemic (left-*M* and right-*P*) helical chains through the hydrogen bonding between $CoCl_4^{2-}$ anion and the 4-fluoro-*α*-phenylethylammonium cations were observed. Here, both the enantiomers are present on the opposite side of the screw axis cancelling out the overall polarity, and therefore no resolution of the 4-fluorophenyleneethyl ammonium cations occurs through crystallization. While in the case **1*R*** and **1*S*,** hydrogen bonding interactions involving the additional Cl^- anion resulted synthos A and C, which in turn resulted in the spontaneous resolution of the racemic 4-chloro-*α*-phenylethyl-ammonium cations.

To understand more on these lines, we have also synthesized separately **1*R*** and **1*S*** using (*R*)-4-chlorophenylethyl ammonium chloride and (*S*)-4-chloro-*α*-phenylethyl ammonium chloride, respectively. The independently synthesized products were identical to conglomerate crystals isolated from the synthesis using the racemic salt on the basis of single crystal X-ray diffraction data. Thus, these results unambiguously demonstrate the spontaneous resolution of *racemic* 4-chlorophenyleneethyl ammonium chloride during complexation with cobalt(II) chloride.

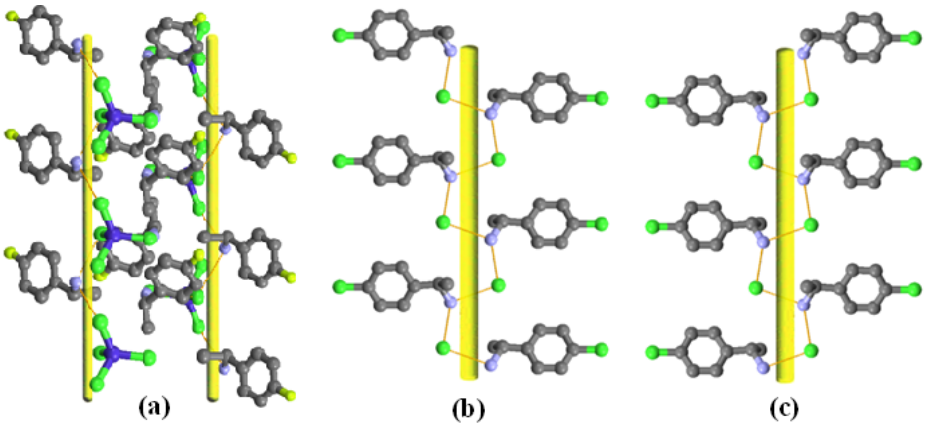

Fig. 5.7: Helical chains of compounds (a) 2-*racemicP*+*M*, (b) 1*R*–*M*,and (c) 1*S*-*P*. Hydrogen atoms and $CoCl_4^{2-}$ are omitted for clarity

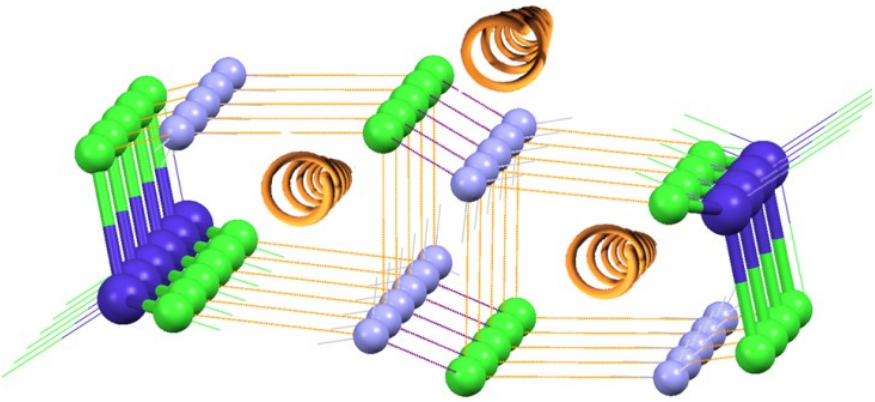

Fig. 5.8: Adjacent helices (opposite in direction) generated by 2-fold screw symmetry operations along the *b*-axis in case of compounds 1*R* and 3*R* while opposite in case of 1*S*

Furthermore this made to realize a correlation between the helicity of 1-D chains and the chirality of ligands as *R*-isomer give left handed structures while *S*-isomer right handed ones. The hydrogen bonded chain is helically folded and extended along the *b*-axis with a helical pitch of 7.554Å for **1*R*** and 7.598 Å for **1*S***, while it is 7.178 Å but along *a*-axis for compound **2**. In each helix of **1*R*** and **1*S*,** two 1-(4-chlorophenyl) ethyl ammonium cations and two chloride ions constitute one turn. The groove of the helical chain is intercalated by one $CoCl_4^{2-}$ and one 1-(4-chlorophenyl)ethyl ammonium cation units belonging to two adjacent helices (opposite in direction) generating 2-fold screw symmetry along the *b*-axis (Figure 5.8). This packing stabilizes the helical structure and is possible only in the presence of a free chloride ion and synthons A and C. We are presently involved in understanding which is more 'dominating' character, synthon or chloride anion incorporation?

In a preliminary investigation in this direction, we subjected enantiomerically pure (*R*)-(+)-1-(phenyl) ethylamine to the self-assembly process with $CoCl_2$, and obtained the "chloride-inclusive" compound $[(R)\text{-}(+)\text{-}C_6H_5CH(CH_3)NH_3)]_3[CoCl_4]Cl$ (**3*R***). Crystal structure determination confirms inclusion of chloride anion and synthons A and C together. This results in spontaneous resolution due to helical chain formation between free chloride anion and 1-(phenyl)ethylammonium cation. Here, the hydrogen bonded helical chain is observed along the *b*-axis with a helical pitch of, 7.503Å similar to **1*R*/1*S*.** Using symmetry elements and Flack parameters, one can comment on the enantiomeric purity of the observed structures. To prove that compound is 100% enantiomerically

excess, flack parameters must be close to zero [19]. Standard uncertainty (u) of flack parameter x (u) should be small and less than 0.04. This uncertainty relaxed up to 0.10 if proven by other techniques as enantiomerically pure.

Compound **2** crystallizes into centrosymmetric space group ($P\bar{1}$) contains an inversion centre, confirming presence of both opposite enantiomeric amines at opposite sites and hence is a racemic mixture. Crystals of **1*R***, **1*S*** and **3*R*** belong to the noncentro-symmetric space group ($P2_1$) and contain 2_1 screw axis rotations, which made determination of absolute configuration feasible. Compound **1*R*** and **3*R*** showed uncertainty 0.07 and 0.10 respectively, which lie in the range of 0.04-0.10 of standard uncertainty (u). **1*S*** showed slightly higher value, 0.14, than the standard range of standard uncertainty value (u) but have small value of x can be correlated to absolute-structure determination [20]. Enantiomeric control during crystallization can be induced by the *pseudo*-seeding with a crystal of desired chirality is under investigation [21].

Table 5.2: Selected bond lengths, bond angles and hydrogen bonds for 1*R*, 1*S*, 2 and 3*R*

Compounds	Co-Cl Dist.	Co-Co Dist.[Å] Inter	Co-Co Dist.[Å] Intra	Cl-Co-Cl Angle [º]	C···X Dist. [Å]	N-H···Cl Dist. [Å]	N-H···Cl Angle[°]
	2.2890(4)	15.587	7.581	115.383(16)	1.7385(18)	3.2377(14)	150.9
	2.2931(4)			110.357(15)		3.3685(13)	114.3
1*R*	2.2578(4)			110.463(15)		3.3663(15)	150.0
	2.2689(4)			104.672(15)		3.2894(14)	120.1
				115.383(16)		3.2894(14)	174.0
				110.623(14)		3.2256(16)	162.1
				105.022(15)		3.3697(14)	151.6
						3.1935(16)	174.6
						3.1592(16)	178.6
						3.1982(15)	157.2
						3.1096(14)	164.2
	2.2647(8)	15.598	7.598	110.24(3)	1.727(4)	3.217(3)	152.8
	2.2870(8)			114.36(4)		3.113(3)	156.8
1*S*	2.2586(9)			111.11(3)		3.170(3)	170.5
	2.2921(9)			105.10(4)		3.382(3)	158.0
				110.14(3)		3.214(3)	162.0
				105.58(3)		3.252(3)	159.1
						3.411(3)	142.7
						3.304(3)	128.8
						3.262(3)	149.7
						3.434(3)	114.1
						3.184(3)	165.0
	2.2689(5)	14.234	7.178	107.63(2)	1.368(3)	3.2989(19)	171.0
	2.2827(5)			112.47(2)		3.365(2)	148.0
2	2.2706(5)			107.737(19)		3.2379(18)	110.0
	2.2556(5)			109.02(2)		3.311(2)	160.0
				109.872(19)		3.465(2)	115.2
				110.058(19)		3.2534(19)	177.2
						3.2348(18)	165.3
						3.4027(17)	110.2
						3.3076(19)	136.3
						3.3563(19)	137.3
	2.2895(5)	14.406	7.503	110.78(2)	NA	3.1707(16)	164.1
	2.2515(6)			106.08(2)		3.130(2)	171.9
3*R*	2.2906(6)			111.07(2)		3.0951(18)	153.7
	2.2670(5)			112.66(2)		3.2889(19)	151.7
				110.03(2)		3.1959(18)	162.0
				106.06(2)		3.226(2)	163.7
						3.2541(19)	156.8
						3.1820(18)	168.0
						3.3163(19)	120.4
						3.321(2)	149.8

CCDC No. 916614, 916613, 916616 and 916615, contains the crystallographic data for the compounds **1*R***, **1*S***, **2** and **3*R*** respectively. This data can be obtained free of charge via http://www.ccdc.cam.ac.uk/conts/retrieving.html, or from the Cambridge Crystallographic Data Centre, 12 Union Road, Cambridge CB2 1EZ, UK; fax: (+44) 1223 336 033; or e-mail: deposit@ccdc.cam.ac.uk.

5.6 Conclusion

- Synthesized four different Cobalt based complexes of general formula (R-$NH_3)_nCl_xCoCl_4$, [where, R-NH_3 = (*R*)- (+)-4-chloro methyl benzylamine (**1*R***) and (*S*)- (-)-4-chloro methyl benzylamine (**1*S***), (±) 4-fluro methyl benzylamine (**2**), (*R*)- (+)- methyl benzylamine (**3*R***),; x= 0, 1 and n=2, 3]
- All the compounds were characterized using elemental analysis, FT-IR, thermal analysis and single crystal X-ray diffraction.
- Isolated structures were observed in complexes, where $CoCl_4^{2-}$ exists in distorted tetrahedral geometry.
- Single crystal studies shows racemic((*R/S*)-(+/-) 4-F-$C_6H_4CH(CH_3)NH_3$, **2**, react with $CoCl_2$ to form two separate anti-parallel helical chains of Cl···NH hydrogen bonding originated in one $[CoCl_4]^{2-}$ tetrahedra with synthon B.
- Single crystal studies on compound **3*R*** [(*R*)-(+)-$C_6H_4CHCH_3NH_3]_3ClCoCl_4$ and **1*R*/1*S*** [(*R/S*)-(+/-)-4-Cl-$C_6H_4CH(CH_3)NH_3]_3ClCoCl_4$ showed presence of free anion Cl^- driving Cl···N interaction in the form of synthons A and C, for separation of racemic amines with conglomerates.
- Due to 'inclusion' of free Cl^- in the structures **1*R*/1*S*** stabilization and continuous formation of helical chains resulted in separation of isomers and hence resolution of racemic mixture of ligand.
- Present work of Cl^- inclusion, leading to novel synthon formation, will help in revealing 'molecular' aspect of controlling helicity and resolution of chiral amines.

Part II

A case study of Cu-azide bridged compounds with *racemic* auxiliary ligand

Abstract:

In this chapter (part II), we have synthesized five copper based compounds with a general formula $[Cu\ (mba)_2\ (N_3)_6]_n$ and $[Cu\ (mba)_2\ (N_3)_2]_n$ by the reaction between $Cu(NO_3)_2 \cdot 3H_2O$, sodium azide with *racemic* methyl benzylamine and/or *racemic* 4-chloro methyl benzylamine in methanol. Compounds **3**, **4** and **6**, **7** were obtained in enantiomerically pure form with (±) - methyl benzylamine (**3-4**) and (±)-4-chloro methyl benzylamine (**6-7**), respectively. Crystals of **5** showed presence of both enantiomers of (±) - methyl benzylamine. Spontaneous resolution had occurred in these compounds and results into conglomerate formation. *Racemic* methyl benzylamine ligand crystallized in 2D azido based complexes while *racemic* 4-chloro methyl benzylamine crystallizes into 1D azido based complexes. 2D system affords three kinds crystals; two of them are chiral crystals i.e. conglomerates (space group $P2_12_12_1$) and one is *racemic* crystals (*Pbca*) in methanol. 1D system affords only conglomerate formation due to strong hydrogen bonding and other supramolecular interactions. All complexes were isolated and characterized by X-ray crystallography and circular dichroism (CD).

Compound **3** and **4** (enantiomers of methyl benzylamine) crystallized in chiral orthorhombic space group $P2_12_12_1$with cell dimensions a = 6.025(8) Å, b = 16.660(2) Å, c = 26.162(4) Å, V = 2624.2(6) $Å^3$ and Z = 8. Compound **5** crystallized in non chiral orthorhombic space group *Pbca* with cell dimensions a = 16.496(4) Å, b = 5.996(3) Å, c = 26.121(6) Å, V = 2584(10) $Å^3$ and Z = 8, with presence of both enantiomers (methyl benzylamine). Compound **6** and **7** (enantiomers of 4-chloro methyl benzylamine) are crystallized in monoclinic crystal system with chiral (polar) space group $P2_1$, having unit cell dimensions for **6** a=11.583(6) Å, b = 7.281(5) Å, c = 12.781(2) Å, β = 110.13(3)°, V = 1031.71(4) $Å^3$ and Z = 2; for **7** a = 11.734(6) Å, b = 7.294(5) Å, c = 12.692(2) Å, β = 110.043(6)°, V = 1019.34(5) $Å^3$ and Z = 2.

5.7 Experimental

5.7.1 Materials and Methods:

All chemicals and solvents were of analytical grade reagents. *rac*-(±) methyl benzyl amine (*rac*)- (±)- 4-chloro-α-methyl benzylamine, and copper (II) chloride were from Aldrich; methyl alcohol (Qualigens) were used without further purification.

5.7.2 Syntheses of Compounds:

A general methodology of azide complexes preparation/syntheses is mentioned in scheme-5.3 and 5.4.

Scheme: 5.3

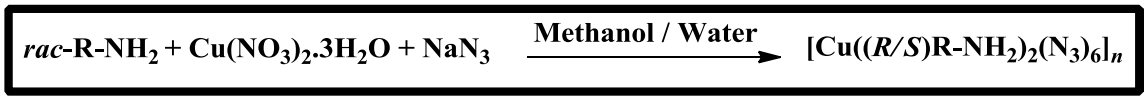

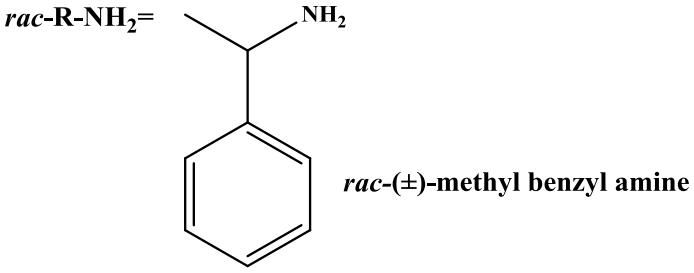

(1)

Scheme: 5.4

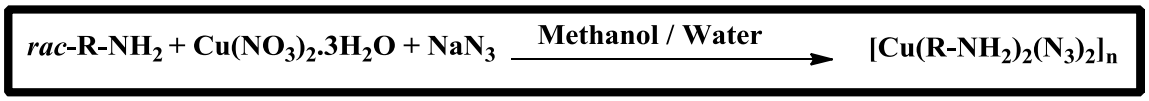

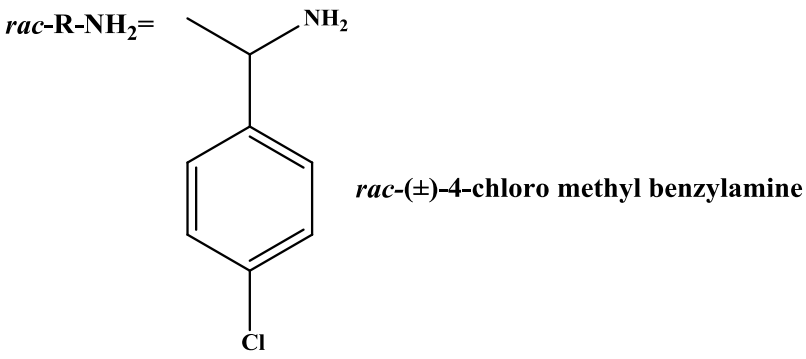

(2)

A methanolic solution (10 mL) containing copper (II) nitrate trihydrate (0.2 mmol) was mixed with an aqueous solution of sodium azide (130 mg, 2 mmol) dissolved in a minimum volume of water. Auxillary ligand amine (**1**) (0.1 mmol) in 3 mL of methanol was added to this reaction mixture with continuous stirring. The resulting dark-green solution was filtered and left to stand at room temperature. Dark green plate-shaped crystals (scheme-5.2) of **3-5** suitable for X-ray diffraction were obtained by slow evaporation of the solvents within 1 week.

Overall yield of single crystals: ~45%

Dark green needle like crystals (scheme-5.3) of compound **6** and **7** were obtained using a similar method to that of **3-5**, except that auxillary ligand amine (**2**) was used (scheme 5.3).

Overall yield of single crystals:~ 55%.

Appearance and morphology of all crystals obtained from scheme-5.3 and scheme-5.4 were similar with no observable difference under microscope.

5.8 Result and Discussions

5.8.1 FT-IR:

Figure 5.9 shows the FT-IR spectra of compounds **3/4** and **5** while Figure 5.10 shows FT-IR spectra of compound **6** and **7**. The data of chiral complexes of 4-Cl methyl benzylamine and methyl benzylamine is already discussed in chapter 2 hence only data of compound **5** presented here. Racemic (**5**) and enantiomeric (**3/4**) do not show any significant change in FT-IR spectra.

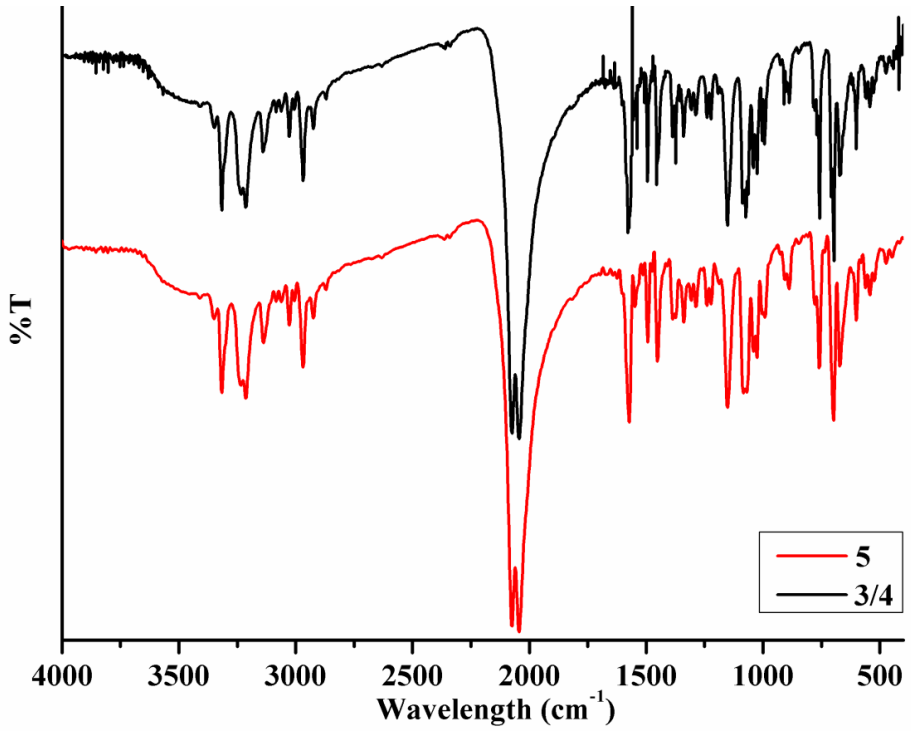

Fig. 5.9: FT-IR spectra of compound 3/4 and 5

Compound 5: FT-IR (KBr pellet, 4000–400 cm^{-1}): 3229 (w), 3061(w),2982 (m), 2933(m), 2080(s), 2052(s), 1609 (s), 1561(s), 1502(s), 1431 (s), 1349(s), 1214(s), 1072(s), 1024(s), 930(m), 812 (s).

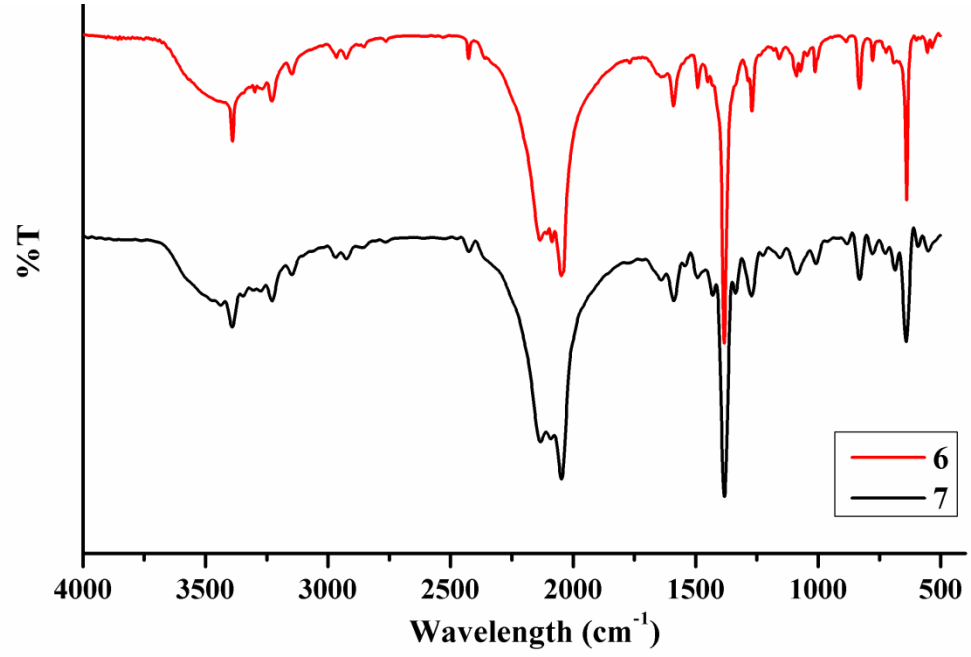

Fig. 5.10: FT-IR spectra of compound 6 and 7

R–NH_2 symmetric and antisymmetric stretching observed in the range of 3315-3348 cm^{-1} and 3213-3233 cm^{-1}. Aliphatic -CH_3 stretching band observed at 2968cm^{-1}. Strong azide bands observed at the 2075 and 2047 cm^{-1}. C-H ring stretching modes were observed in the range 1455-1604 cm^{-1}. CH_3 symmetric deformation mode observed in the range 1385-1374 cm^{-1} and at 1290 cm^{-1}. Bands in the range 1336-1340 cm^{-1} indicate the C-N stretching mode. *in- plane* C-H deformation modes were observed in the range 1028-1240 cm^{-1} while C-C *stretching* mode was observed in the range 970-994cm^{-1}. Bands in the range 910-916 cm^{-1} was attributed to -CH_2 *rocking* mode. Sharp bands were observed at 749-770 cm^{-1} assigned to the *out-of- plane* ring deformation. Out-of-plane C-H deformation modes were observed around 698-747 cm^{-1}.

5.8.2 Elemental Analyses:

The calculated elemental analyses were consistent with the observed formulae of azide complexes.

Compound 3: Anal. Calc. for $C_{16}H_{22}Cu_3N_{20}$: C, 28.05; H, 3.24; N, 40.89%. **Found:** C, 27.80; H, 3.30; N, 40.65%.

Compound 4: Anal. Calc. for $C_{16}H_{22}Cu_3N_{20}$: C, 28.05; H, 3.24; N, 40.89%. **Found:** C, 27.85; H, 3.38; N, 40.59%.

Compound 5: Anal. Calc. for $C_{16}H_{22}Cu_3N_{20}$: C, 28.05; H, 3.24; N, 40.89%; **Found:** C, 27.86; H, 3.37; N, 40.63%.

Compound 6: Anal. Calc. for $C_{16}H_{20}Cl_2CuN_8$: C, 41.84; H, 4.35; N, 24.40%. **Found:** C, 41.02; H, 4.29; N, 24.70%.

Compound 7: Anal. Calc. for $C_{16}H_{20}Cl_2CuN_8$: C, 41.84; H, 4.35; N, 24.40%; **Found:** C, 41.18; H, 4.31; N, 24.31%.

5.9 Crystal structure

The molecular structure of **3, 4** and **5** are shown in Figure 5.11 (a, b, and c) while molecular structure of compound **6** and **7** shown in Figure 5.12. Refinement parameters for all compounds are given in Table 5.3.

Table 5.3: Crystal structure and refinement parameters for compounds 3, 4, 5, 6 and 7

	3	4	5	6	7
Empirical formula	$C_{16}H_{22}Cu_3N_{20}$	$C_{16}H_{22}Cu_3N_{20}$	$C_{16}H_{22}Cu_3N_{20}$	$C_{16}H_{20}Cl_2CuN_8$	$C_{16}H_{20}Cl_2CuN_8$
Formula weight	685.19	685.19	685.19	458.84	458.84
Wavelength	0.71073 Å	0.71073 Å	0.71073 Å	0.71073 Å	0.71073 Å
Crystal system	Orthorhombic	Orthorhombic	Orthorhombic	Monoclinic	Monoclinic
Space group	$P2_12_12_1$	$P2_12_12_1$	*Pbca*	$P2_1$	$P2_1$
Unit cell dimensions	a = 6.0249(8)Å b =16.660(2)Å c = 26.145(4)Å α= β = γ = 90°	a = 6.0321(6)Å b =16.693(5)Å c = 26.162(2)Å α= β = γ = 90°	a = 16.496(4)Å b =5.996(13)Å c = 26.121(6)Å α= β = γ = 90°	a = 11.583(6)Å b = 7.281(5) Å c = 12.781(2) Å β = 110.13°	a = 11.734(6)Å b =7.294(5)Å c = 12.692(2)Å β = 110.04º
Volume	2624.2(6) $Å^3$	2620.8(6) $Å^3$	**2584.06(10)$Å^3$**	1031.71(4) $Å^3$	1019.34(5) $Å^3$
Z	8	8	8	2	2
Density (calculated)	1.734 Mg/m^3	1.729Mg/m^3	1.751Mg/m^3	1.412 Mg/m^3	1.412 Mg/m^3
Absorption coefficient	2.459 mm^{-1}	2.356mm^{-1}	3.300 mm^{-1}	1.359 mm^{-1}	1.346mm^{-1}
Reflections collected	14026	13598	5472	5681	5234
Independent reflections	5156 [R_{int} = 0.0523	5188 [R_{int} = 0.0518	2472 [R(i nt) = 0.0325]	4329 [R_{int} = 0.0323	3791 [R_{int} = 0.0259
Refinement method	Full-matrix least-squares on F^2	Full-matrix least-squares on F^2	Full-matrix least-squares on F^2	Full-matrix least-squares on F^2	Full-matrix least-squares on F^2
Data / restraints / parameters	5156/0/354	5188/0/351	2472/0/179	4321/0/354	3825/0/257
Goodness-of-fit on F2	1.089	1.076	1.041	0.987	1.112
Final R indices [I>2sigma(I)]	R_1 = 0.0651, wR_2 = 0.1365	R_1 = 0.0636, wR_2 = 0.1357	R1 = 0.0492 wR2 = 0.1224	R_1 = 0.0412, wR_2 = 0.0865	R_1 = 0.0427, wR_2 = 0.0912
R indices (all data)	R_1 = 0.0895, wR_2 = 0.1425	R_1 = 0.0892, wR_2 = 0.1429	R1 = 0.0597 wR2 = 0.1300	R_1 = 0.0567, wR_2 = 0.0928	R_1 = 0.0451, wR_2 = 0.0956

Chapter 2 discussed 1D molecular magnets where direction of helicity or CAL-CAL was driven by enantiomeric nature of ligand. To verify similar effect on racemic ligand for the final 1D and 2D structures we have carried out crystallization of racemic auxillary ligand 4-chloro-α-methyl benzylamine and α-methyl benzylamine. We observed conglomerate formation in both the cases, along with formation of racemic crystal structure in case of former only.

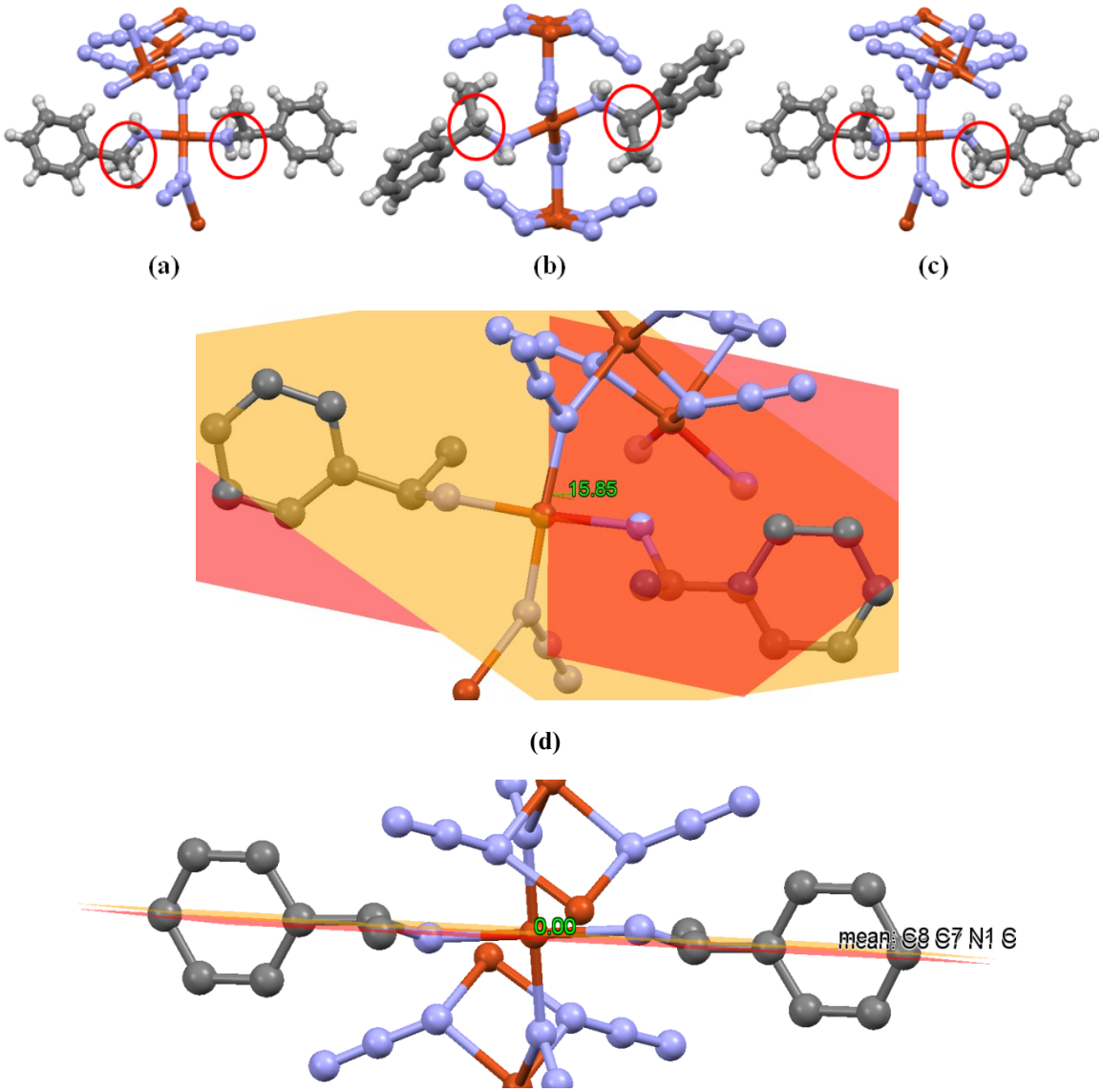

(a) (b) (c)

(d)

(e)

Fig. 5.11: (a) Compound 3(*R*), (b) Compound 5 (*RS*), (c) Compound 4 (*S*); Red circles indicate the chiral centers (d) & (e) Dihedral Angle between two ligands of compound 4 (*S*)- 15.85° and 5 (*RS*)- 0.00°

Chiral auxillary ligand (*R/S*)-*α*-methyl benzylamine crystallizes in orthorhombic chiral space group $P2_12_12_1$ ($[Cu_3((R)\text{-mba})_2\text{-}(N_3)_6]_n$(**3**) and $[Cu_3((S)\text{-mba})_2(N_3)_6]_n$(**4**)), is reported in the literature[22]. These complexes were prepared using enantiomerically pure starting compounds. Self-assembly formation of compound **3** and **4** formed neutral 2D brick-wall layers with a repeating azido-bridged eight membered copper brick [6.025(8) Å]. Here Cu was found to exist in three crystallographically different environments, two with square pyramidal in which each one coordinated with five *EO* azide bridge and one with square planar geometry coordinated with nitrogen of two ligands and two *EE* azide bridge.

When racemic (±)-*α*-methyl benzylamine ligand was used instead of enantiomerically pure ligand, self-assembly formation leads to resolution with enantiomerically pure crystals as well as racemic crystals. The *conglomerates* compounds **3** and **4** are crystallized into the $P2_12_12_1$ acentric space group similar to reported one while the *racemic* compound **5** into centrosymmetric *Pbca* space group. Figure 5.10 a, b, and c show structure for ($[Cu_3((R)\text{-mba})_2\text{-}(N_3)_6]_n$ (**3**) and $[Cu_3((S)\text{-mba})_2(N_3)_6]_n$ (**4**)) *racemic* complex ($[Cu_3((rac)\text{-mba})_2(N_3)_6]_n$ (**5**), respectively.

Table 5.4: Selected bond length of compounds 3/4 and 5

Bond length	Reported (3 and 4)	Compound 5
Cu1--- Cu3	4.169	4.099
Cu2(1)--- Cu3	3.038	3.012
Cu2(2)--- Cu3	3.015	3.012
Cu2(#2)--- Cu3	8.275	8.197
Cu1---N1	2.007	2.007
Cu1---N2	2.023	2.007
Cu1---N18	2.013	2.012
Cu1---N3	2.025	2.012

Table 5.5: Selected bond angles of compounds 3/4 and 5

Bond angle	Reported (3 and 4)	Compound 5
Cu1-N18- Cu3	137.15	134.38
Cu2(#2)-N3-Cu1	132.65	134.38
Cu2(1)-N12- Cu3	96.26	96.97
Cu2(1)-N15- Cu3	101.84	99.14
Cu2(2)-N6- Cu3	100.08	96.97
Cu2(2)-N9- Cu3	98.20	99.14
N2-Cu1-N1	171.51	180.00
N18-Cu1-N3	175.51	180.00
N18-N19-N20	171.98	174.81
N3-N4-N5	175.65	174.81
N6-N7-N8	177.01	179.27
N9-N10-N11	175.41	178.14
N12-N13-N14	176.58	179.27
N15-N16-N17	176.13	178.14

Looking close into the crystal structure, we observed that the dihedral angle between two ligand vary in chiral compound **3**/ **4** (0º) and in racemic compound **5** (15.85º) as shown by red circles in Figure 5.11-a, b, c. In compound **5** the *R* and *S* isomer ligands are crystallized into the same crystal causing perfectly square planar geometry around copper metal (Table 5.5).

All bond distances and bond angles of compound **5** are varied from $P2_12_12_1$ acentric crystals (**3/4**) (Table 5.4 -5.5). Compound **5** does not showed any observable strong hydrogen bond or van der Wall interaction due to which the twisting of ligand and crystallization of opposite isomer has occurred. The two phenyl rings twist around

–CH(CH_3)−NH_2 group with different bond angles for geometry around Cu(II) centers. The angles became same of Cu-azido linkage $[Cu((rac)\text{-mba})_2]^{2+}$ units through the EO azido bridges [Cu-N_{EO}-Cu, 134.3(8)°], because of shorten distance between two layers causing decreased in crystal volume by 1.53% compared to crystal volume of **3/4** (Table 5.3) in accordance with literature. The reduced distance between two neutral two-dimensional (2D) brick-wall layers is 8.197Å which allows the rotation of ligand phenyl ring. According to Wallach *et. al*., [23] crystals of racemates tend to be more densely packed than their chiral counterparts and escaping of tight packing results in the formation of conglomerates.

Racemic ligand, 4-chloro-*α*-methyl benzylamine, gave only conglomerate crystals of **6** and **7** with right handed and left handed helical chains as shown in Figure 5.12. X-ray crystallography revealed that **6** and **7** are enantiomers and crystallized into the chiral space group $P2_1$ in which Cu^{II} ion is five nitrogen coordinated in the form of a distorted square based pyramid, CuN_5. The axial position is occupied by one nitrogen atom N(6) of the azide bridge in the EE mode ($Cu1\text{-}N6_{axial}$; 2.333-2.377 Å) and the equatorial plane is formed by nitrogen atoms from the two isomeric 4-chloro-*α*-methyl benzylamine ligands (Cu1-N1;1.997-2.011 Å , Cu1- N2;2.001-2.013 Å) and the nitrogen atom of the EO azide (Cu1- N3; 2.006- 2.009Å). Here *R* as well as *S* isomers of ligands gets resolved into separate crystals and crystallized to give one dimensional helical azido networked. The helicity depends upon the resolved enantiomeric isomers of ligand. Due to strong hydrogen bonding and supramolecular interactions only conglomerate formation has occurred.

The supramolecular inter-chain weak Cl---N (3.239 Å; C(3)-Cl(1)-N(5): 146.47) interaction along crystallographic c-axis between the chlorine and terminal nitrogen atom of the EO azide is observed (Figure 5.13-a, b). Because of this interaction the racemic product is not observed, a distinct change with respect to **5** from auxillary ligand **1**. This supramolecular interaction stabilizes the helical chains due to which the crystallization of opposite enantiomeric ligand and rotation of phenyl ring of auxillary ligand hindered. Chirality of *R* and *S* isomer of compound **6** and **7** is induced by the self assembly

formation and driven by coordination around the metal center, ligand flexibility, and supramolecular interactions.

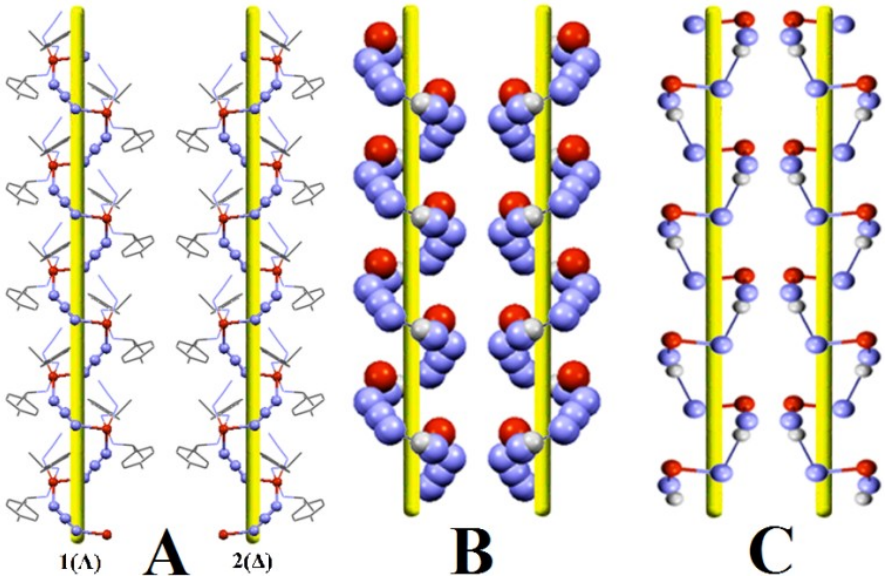

Fig. 5.12: 1D Left handed (Λ) and Right (Δ) handed helical chains along 2_1 screw axis for 6 and 7, respectively, showing (A) EE-azide network between Cu(II) ; (B) & (C) hydrogen bonding between N-H amine

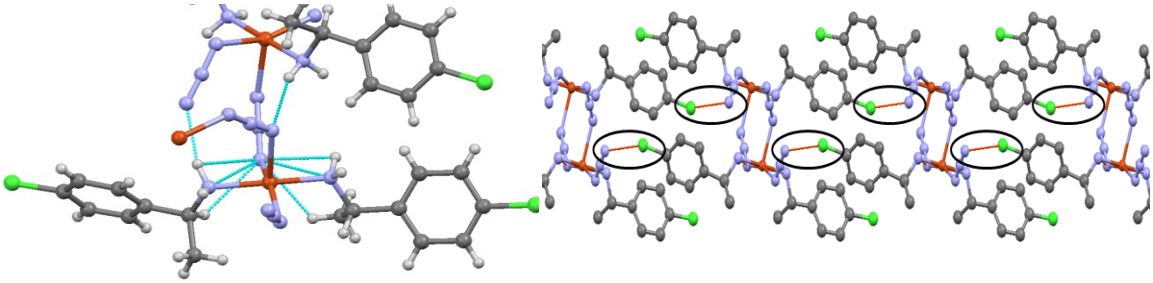

(a) **(b)**

Fig. 5.13: (a) Rotation hindered due to Strong H-bonding of Ligand and azide (b) Supramolecular Cl···N interactions (Cl···N = 3.239 Å, blue lines) along the helical chains

The left/right-handed chirality of the helical chain is transferred uniformly to adjacent chains through the interchain supramolecular interactions, resulting in the formation of homochiral arrangements in the crystals as shown in Figure 5.13b.

5.10 CD Spectra

The absolute configurations of individual crystals of *R* and *S* were further confirmed using solid-state circular dichroism (CD) spectroscopy. Furthermore in case of 4-chloro-α-methyl benzylamine complexes, compound **5**, no visible CD signal was obtained for the bulk sample indicating two enantiomers in 1: 1 ratio.

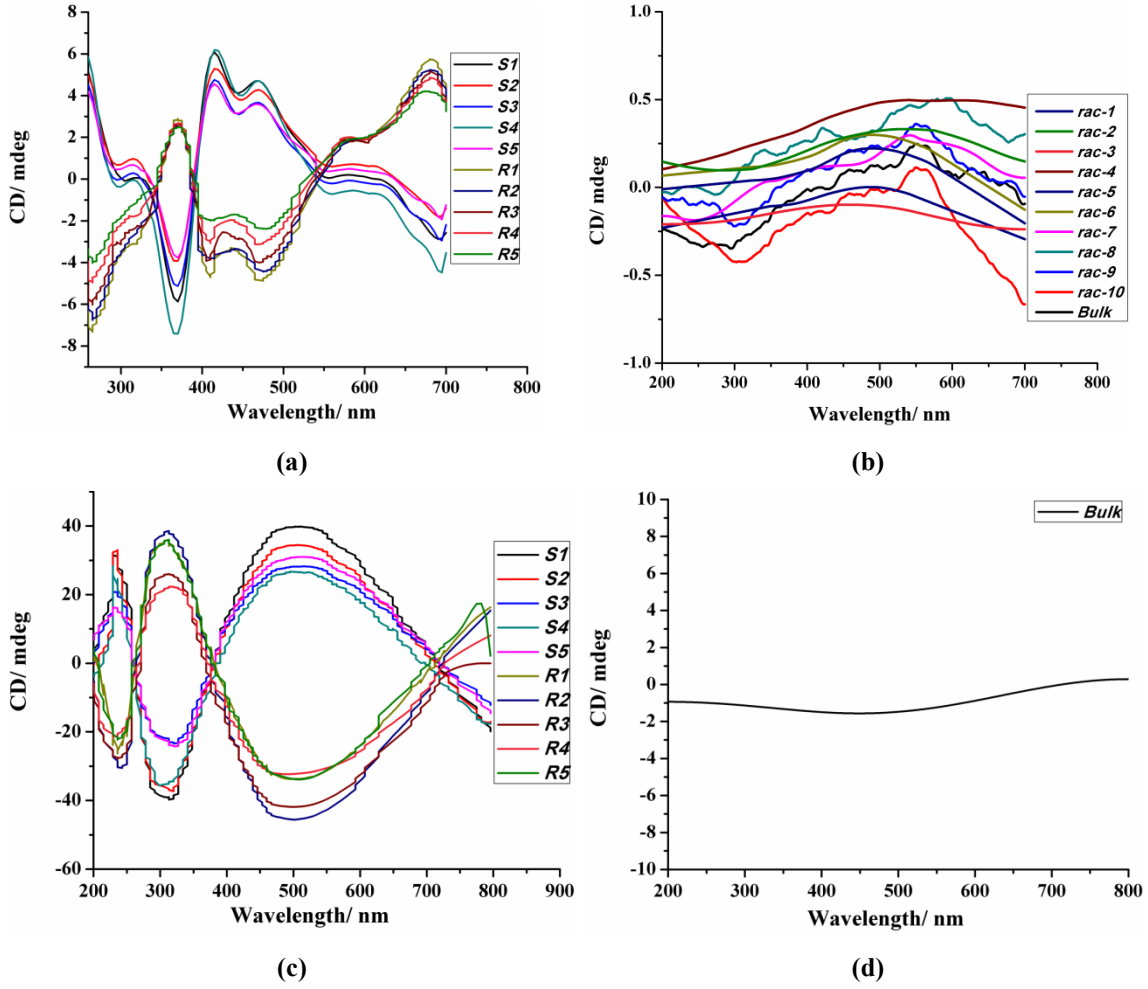

Fig. 5.14: (a)Solid CD spectra of 3 (*R*1-*R*5) and 4 (*S*1-*S*5) in nujol, (b) Solid CD spectra of compound 5 (*rac*1- *rac* 10) and bulk sample in nujol, (c) Solid CD spectra of 5(*R*1-*R*5) and 6(*S*1-*S*5) in nujol and (d) CD spectra of bulk of sample

Compounds 3, 4 and 5: The circular dichroism (CD) spectra measured in nujol are shown in Figure 5.14-a, c. The crystals were selected after single crystal XRD studies on them. Solid-state CD measurements for the result bulk materials are CD-silent. The static

process produced the expected statistically equal number of **3(*R*)** and **3(*S*)** (right-handed) crystals, and a racemate **5** (*racemic* mixture-*RS*) was obtained.

The spectrum for a single crystal of compound **3(*R*)** in a nujol displays one positive Cotton effects at 365 nm which can be attributed to $\pi \rightarrow \pi^*$ and two negative cotton effect at 405 nm and 460nm while that for compound **3(*S*)** it is nearly mirror image (Figure 5.14a). The racemic crystals i.e. compound **5** showed the silent CD spectrum confirming the crystallization of both isomers in the same crystal (Figure 5.14b). The bulk material also showed silent CD spectrum.

Compounds 6 and 7: Solid-state CD measurements for the resulting bulk materials are CD-silent, indicating two enantiomeric crystals are in nearly 1: 1 ratio (Figure 5.14d). But each individual single crystal was optically active and showed intense CD activity.

Compound **6**(*R*) showed positive Cotton effects at λ_{max} = 232 and 503 nm and negative cotton effect at 299 nm which can be attributed to $\pi \rightarrow \pi^*$ while **7(*S*)** exhibits a negative Cotton effect at λ_{max} =230nm and 506 nm and a positive dichroic signal centered at 300 nm. Furthermore, band at 506 nm in **6** and **7** is assigned to copper (II) *d–d* transition,

To confirm no crystal with both enantiomers, case similar to 5, we randomly picked 10 crystals from the same batch of crystallization. The CD spectrum of each crystal was either matched with **6**(*R*) or **7**(*S*) (Figure 5.14c). Coincidently, we observed exactly five crystals with **6**(*R*) and **7**(*S*) CD activity. The results confirm each crystal is spontaneously resolved by crystallization.

5.11 Conclusion

- Racemic auxillary ligands, *racemic* methyl benzylamine **1** and *racemic* 4-chloro methyl benzylamine **2** gives 2D and 1D copper azido complexes respectively.
- All compounds were characterized using elemental analyses, FT-IR, CD spectroscopy and Single Crystal X-ray Diffraction.
- Spontaneous resolution of auxillary racemic ligand **1** results in to formation of conglomerate crystals (**3** and **4**) having chiral space group $P2_12_12_1$ as well as racemic crystal (**5**) having non chiral space group *Pbca*.
- In all compound (**3**, **4** and **5**) copper was found to exist in three different crystallographically environments (two square pyramidal and one square planar).
- Crystallization of racemic compound **5** (copper azido complex) happens due to square planar geometry around copper and phenyl rings twist.
- Only conglomerates (**6** and **7**) formation occurred in case of spontaneous resolution of auxillary ligand **2**.
- Compound **6** and **7** crystallized into chiral space group $P2_1$ in which copper having only square pyramidal geometry.
- Strong hydrogen bonding and supramolecular interactions (Cl---N) prohibit the crystallization of opposite isomer in **6** and **7** and hence resulting into conglomerates only and not racemic complex.
- CD spectra confirm the enantiomeric nature of the optically active compounds i.e. compounds **3**, **4**, **6** and **7**.
- Compound **5** showed silent CD spectra confirm the crystallization of both isomers.
- Overall work can be schematically represented in Scheme 5.4.

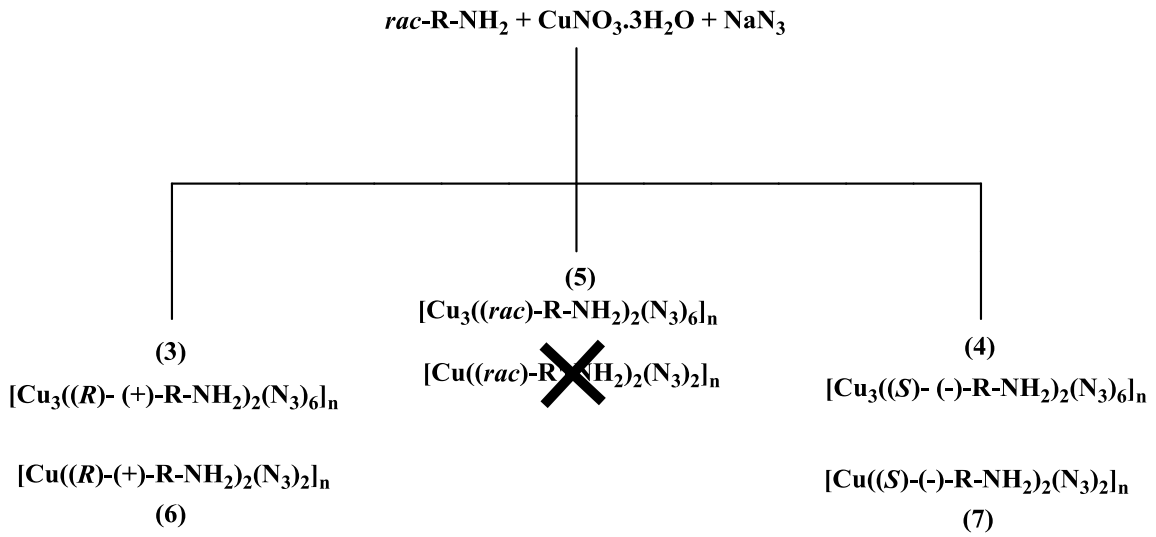

Scheme 5.4: Schematic representation of compound formation

5.12 References

[1] (a) J. S. Seo, D. Whang, H. Lee, S. I. Jun, J. Oh, Y. J. Jeon, K. Kim, *Nature* **2000**, *404*, 982-986; (b) R.-G. Xiong, X.-Z. You, B. F. Abrahams, Z. Xue, C.-M. Che, *Ang. Chem. Int. Ed.* **2001**, *40*, 4422-4425; (c) J. J. Bodwin, A. D. Cutland, R. G. Malkani, V. L. Pecoraro, *Coord. Chem. Re*v. **2001**, *216–217*, 489-512; (d) B. Kesanli, W. Lin, *Coord. Chem. Re*v. **2003**, *246*, 305-326; (e) A. Hu, H. L. Ngo, W. Lin, *J. Am. Chem. Soc.* **2003**, *125*, 11490-11491; (f) A. Hu, H. L. Ngo, W. Lin, *Angew. Chem., Int. Ed.***2004**, *43*, 2501-2504.. (h) J. Hua, W. Lin, *Org. Lett.* **2004**, *6*, 861-864; (i) A. Hu, H. L. Ngo, W. Lin, *Angew. Chem., Int. Ed.* **2003**, *42*, 6000-6003; (g)C.-D. Wu, A. Hu, L. Zhang, W. Lin, *J. Am. Chem. Soc.* **2005**, *127*, 8940-8941; (h) C.-D. Wu, W. Lin, *Angew. Chem. Int. Ed.* **2005**, *44*, 1958-1961;(i) C.-D. Wu, W. Lin, *Inorg. Chem.* **2005**, *44*, 1178-1180;(f) B. Kesanli, W. Lin,*Chem. Commun.* **2004**, 2284-2285; (j) A. Hu, G. T. Yee, W. Lin, *J. Am. Chem. Soc.* **2005**, *127*, 12486-12487.

[2] (a) E.-Q. Gao, S.-Q. Bai, Z.-M. Wang, C.-H. Yan, *J. Am. Chem. Soc.***2003**, *125*, 4984-4985; (b) E.-Q. Gao, Y.-F. Yue, S.-Q. Bai, Z. He, C.-H. Yan, *J. Am. Chem. Soc.***2004**, *126*, 1419-1429; (c) H.-R. Wen, C.-F. Wang, Y. Song, J.-L. Zuo, X.-Z. You, *Inorg. Chem*. **2005**, *44*, 9039-9045; (d) E. Coronado, J. R. Galán-Mascarós, C. J. Gómez-García, E. Martínez-Ferrero, M. Almeida, J. C. Waerenborgh, *Eur. J. Inorg. Chem.***2005**, *2005*, 2064-2070.

[3] (a) B. J. Coe, N. R. M. Curati, *Comm. Inorg. Chem.***2004**, *25*, 147-184; (b) L.-L. Wen, D.-B. Dang, C.-Y. Duan, Y.-Z. Li, Z.-F. Tian, Q.-J. Meng, *Inorg. Chem.* **2005**, *44*, 7161-7170; (c) S. Galli, N. Masciocchi, E. Cariati, A. Sironi, E. Barea, M. A. Haj, J. A. R. Navarro, J. M. Salas, *Chem. Mater.* **2005**, *17*, 4815-4824; (d) Q. Ye, Y.-H. Li, Q. Wu, Y.-M. Song, J.-X. Wang, H. Zhao, R.-G. Xiong, Z. Xue, *Chem. Eur. J.* **2005**, *11*, 988-994.

[4] (a) H. M. Mande, P. S. Ghalsasi, N. Arulsamy, *Cryst. Growth Des.* **2014**, *14*, 4254-4257; (b) J. Zhang, S. Chen, A. Zingiryan, X. Bu, *J. Am. Chem. Soc.* **2008**, *130*, 17246-17247; (c) F. Song, C. Wang, J. M. Falkowski, L. Ma, W. Lin, *J. Am. Chem. Soc.* **2010**, *132*, 15390-15398 (d) Y. Wen, T. Sheng, S. Hu, X. Ma, C. Tan, Y.

Wang, Z. Sun, Z. Xue, X. Wu, *Chem. Commun.* **2013**, *49*, 10644-10646; (e) K. Mo, Y. Yang, Y. Cui, *J. Am. Chem. Soc.* **2014**, *136*, 1746-1749; (f) L. Pérez-García, D. B. Amabilino, *Chem. Soc. Rev.* **2002**, *31*, 342-356.

[5] J. Jacques, A. Collet and S. H. Wilen, *Enantiomers, Racemates and Resolutions*, Krieger Publishing Company, Malabar, Florida,**1994**.

[6] (a) A. Collet, M. J. Brienne, J. Jacques, *Chem. Rev.* **1980**, *80*, 215-230; (b) J. Jacques, A. Collet, S. W. Enantiomers, Wiley-Interscience publication, New York, **1981**; (c) D. K. Kondepudi, K. Asakura, *Acc. Chem. Res.* **2001**, *34*, 946-954; (d) L. Perez-Garcia, D. B. Amabilino, *Chem. Soc. Rev.* **2002**, *31*, 342-356; (e) M. A. Sephton, C. R. Emerson, L. N. Zakharov, P. R. Blakemore, *Chem. Commun.* **2010**, *46*, 2094-2096.

[7] L. Pasteur, *Ann. Chim. Phys.*, **1848**, *24*, 442-459.

[8] Jacques, J.; Collet, A.; Wilen, S. H. *Enantiomers, Racemates and Resolutions*; Krieger Publishing Co: Malabar, FL, **1994**.

[9] E.-Q. Gao, Y.-F. Yue, S.-Q. Bai, Z. He, C.-H. Yan, *J. Am. Chem. Soc.* **2004**, *126*, 1419-1429.

[10] L. Pérez-García, D. B. Amabilino, *Chem. Soc. Rev.* **2002**, *31*, 342-356.

[11] (a) W. Saenger, in *Principles of Nucleic Acid Structure*, Springer New York, **1984**, pp. 253-282.; (b) J. Steed, J. Atwood, John Wiley & Sons, Chichester, **2000**.

[12] (a) F. Montanari, L. Casella, *Metalloporphyrins Catalyzed Oxidations, Vol. 17*, Springer, **1994**; (b) T. D. James, K. R. A. S. Sandanayake, S. Shinkai, *Angew. Chem. Int. Ed. Engl.* **1996**, *35*, 1910-1922; (c) Y. Furusho, T. Kimura, Y. Mizuno, T. Aida, *J. Am. Chem. Soc.* **1997**, *119*, 5267-5268; (d) T. Verbiest, S. V. Elshocht, M. Kauranen, L. Hellemans, J. Snauwaert, C. Nuckolls, T. J. Katz, A. Persoons, *Science* **1998**, *282*, 913-915; (e) K. Akagi, G. Piao, S. Kaneko, K. Sakamaki, H. Shirakawa, M. Kyotani, *Science* **1998**, *282*, 1683-1686; (f) H. Ogoshi, T. Mizutani, *Acc. Chem. Res.* **1998**, *31*, 81-89; (g) E. Yashima, K. Maeda, Y. Okamoto, *Nature* **1999**, *399*, 449-451; (h) L. J. Prins, J. Huskens, F. de Jong, P. Timmerman, D. N. Reinhoudt, *Nature* **1999**, *398*, 498-502; (i) S. Zahn, J. W. Canary, *Science* **2000**, *288*, 1404-1407; (j) J. S. Seo, D. Whang, H. Lee, S. Im Jun, J. Oh, Y. J. Jeon, K.

Kim, *Nature* **2000**, *404*, 982-986; (k) B. L. Feringa, R. A. van Delden, N. Koumura, E. M. Geertsema, *Chem. Rev.* **2000**, *100*, 1789-1816; (l) B. Kolp, H. Viebrock, A. von Zelewsky, D. Abeln, *Inorg. Chem.* **2001**, *40*, 1196-1198; (m) Y. Okamoto, E. Yashima, C. Yamamoto, in *Materials-Chirality*, John Wiley & Sons, Inc., **2004**, pp. 157-208; (n) I. Stibor, P. Zlatušková, in *Anion Sensing, Vol. 255* (Ed.: I. Stibor), Springer Berlin Heidelberg, **2005**, pp. 31-63; (o) A. Sensing, I. Stibor, *Springer-Verlag, Berlin* **2005**, *255*, 1-238.

[13] T. Ezuhara, K. Endo, Y. Aoyama, *Journal of the American Chemical Society* **1999**, *121*, 3279-3283.

[14] X. J. Luan, Y. Y. Wang, D. S. Li, P. Liu, H. M. Hu, Q. Z. Shi, S. M. Peng, *Angew. Chem., Int. Ed.***2005**, *44*, 3864-3867; (b) X.-C. Huang, J.-P. Zhang, Y.-Y. Lin, X.-M. Chen, *Chem. Commun.* **2005**, 2232-2234; (c) L. Jiang, T.-B. Lu, X.-L. Feng, *Inorg. Chem.* **2005**, *44*, 7056-7062.

[15] (a) R. G. Xiong, X. Z. You, B. F. Abrahams, Z. Xue, C. M. Che, *Angew. Chem., Int. Ed.***2001**, *40*, 4422-4425; (b) J. D. Ranford, J. J. Vittal, D. Wu, X. Yang, *Angew. Chem, Int. Ed.* **1999**, *38*, 3498-3501; (c) J. S. Seo, D. Whang, H. Lee, S. Im Jun, J. Oh, Y. J. Jeon, K. Kim, *Nature* **2000**, *404*, 982-986.

[16] (a) K. Biradha, C. Seward, M. J. Zaworotko, *Angew. Chem, Int. Ed.* **1999**, *38*, 492-495; (b).E.-Q. Gao, S.-Q. Bai, Z.-M. Wang, C.-H. Yan, *J. Am. Chem. Soc.* **2003**, *125*, 4984-4985.

[17] K. Nakamoto, *Infrared and Raman spectra of inorganic and coordination compounds*, Wiley Online Library, **1978**.

[18] (a) D. K. Kumar, A. Das, P. Dastidar, *Cryst. Growth Des.* **2006**, *6*, 216-223; (b) V. Balamurugan, M. S. Hundal, R. Mukherjee, *Chem. Eur. J.* **2004**, *10*, 1683-1690; (c) L. Brammer, E. A. Bruton, P. Sherwood, *Cryst. Growth Des.* **2001**, *1*, 277-290; (d) G. Aullon, D. Bellamy, A. Guy Orpen, L. Brammer, A. B. Eric, *Chem. Commun.***1998**, 653-654.

[19] (a) H. Flack, G. Bernardinelli, *Chirality* **2008**, *20*, 681-690; (b) H. D. Flack, *Helv. Chim. Acta* **2003**, *86*, 905-921; (c) H. Flack, G. Bernardinelli, *J. Appl. Crystallogr.* **2000**, *33*, 1143-1148.

[20] (a) Muller, P.; Riegert, D.; Bernardinelli, G. *Helv Chim Acta,* **2004**, *87*, 227-239;(b) Muller, P.; Nury, P. *Helv Chim Acta*, **2001**, *84*,662-677.

[21]H. Koshima, *J. Mol. Struct*., **2000**, *552*, 111-116.

[22] Z.-G. Gu, Y. Song, J.-L. Zuo, X.-Z. You, *Inorg. Chem.* **2007**, *46*, 9522- 9524.

[23] O. Wallach, *Liebigs Ann. Chem*. **1895**, *286*, 90-118.